

Maximizing Reliability with Bayesian Optimization

Jack M. Buckingham¹ Ivo Couckuyt^{2,3} Juergen Branke⁴

Abstract

Bayesian optimization (BO) is a popular, sample-efficient technique for expensive, black-box optimization. One such problem arising in manufacturing is that of maximizing the reliability, or equivalently minimizing the probability of a failure, of a design which is subject to random perturbations – a problem that can involve extremely rare failures ($P_{\text{fail}} = 10^{-6} - 10^{-8}$). In this work, we propose two BO methods based on Thompson sampling and knowledge gradient, the latter approximating the one-step Bayes-optimal policy for minimizing the logarithm of the failure probability. Both methods incorporate importance sampling to target extremely small failure probabilities. Empirical results show the proposed methods outperform existing methods in both extreme and non-extreme regimes.

1. Introduction

The reliability of a system is quantified by the probability that a design satisfies all performance constraints when that performance depends on random inputs or disturbances. In many applications it is natural to seek to maximize reliability, or equivalently minimize the probability of failure. Examples include yield optimization of electronic components (Wang et al., 2018; Weller et al., 2022), the design of mechanical components (Huang & Chan, 2010; Bichon et al., 2012), the optimization of advertising campaigns (Betei et al., 2024) and the choice of treatment dosage in a medical setting (Durham et al., 1998).

The linear version of this problem was first studied as the ‘P Model’ variant of chance constrained programming by Charnes & Cooper (1963). However, the examples given above are generally non-linear and non-convex, with data

¹Mathsys CDT, University of Warwick, Coventry, UK ²Faculty of Engineering and Architecture, Ghent University, Ghent, Belgium ³imec, Leuven, Belgium ⁴Warwick Business School, University of Warwick, Coventry, UK. Correspondence to: Jack M. Buckingham <jack.buckingham@warwick.ac.uk>, Juergen Branke <juergen.branke@wbs.ac.uk>.

acquisition relying on resource-intensive simulation or real-world experiments.

In some cases, the required reliability is very high, meaning importance sampling or other techniques for estimating rare event probabilities must be applied. For example, in electronics, because millions of SRAM cells are stacked together, the failure rate of an individual cell must be at most $10^{-8} - 10^{-6}$ to ensure a reasonable failure rate for the whole (Sun et al., 2015). Additionally, in both simulations and experiments, gradients are typically unavailable, and we are limited to making a small number of carefully chosen evaluations. Hence, Bayesian optimization (BO) is an ideal algorithm (Frazier, 2018; Garnett, 2023).

Minimizing the failure probability hinges on learning an accurate representation of the relevant parts of the boundary which separates the feasible and infeasible regions. In reliability engineering this is known as the *limit state surface*. Consider the design of a mechanical or electronic component, where it is not possible to exactly manufacture the nominal design and instead the final design is a perturbation of this nominal design. An efficient optimization algorithm would run experiments on designs which are close to both the limit state surface and the nominal design. However, existing methods fail to capitalize on this and instead explore the whole limit state surface evenly. This can be seen in Figure 1, where knowledge gradient (one algorithm proposed in this paper) is compared with an alternative proposed in (Huang & Chan, 2010).

Contributions

1. We propose two acquisition strategies to extend BO to the problem of maximizing reliability, one based on Thompson sampling (called TS-MR) and the other on knowledge gradient (called KG-MR).
2. We provide one approximation for TS-MR, and two approximations for KG-MR, all of which incorporate importance sampling to extend applicability to the regime of extremely small optimal failure probabilities.
3. We demonstrate that both TS-MR and KG-MR outperform the state-of-the-art on many examples, with one-shot KG-MR being the most reliable top performer.

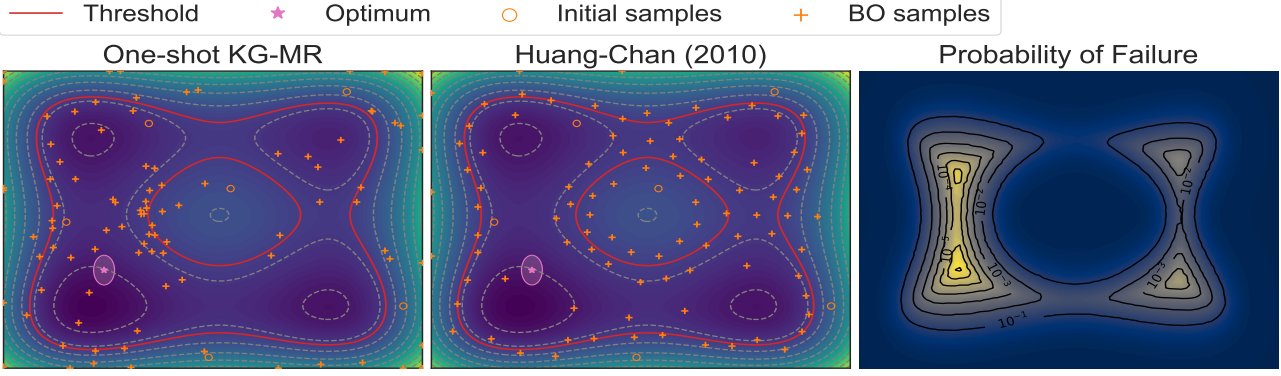


Figure 1. Contour plots showing the Styblinski-Tang (2D) problem where the nominal design is perturbed by adding a normally distributed random variable, and perturbed designs with a value above the threshold are classed as failures. The left and middle panels show the black-box function f and the threshold level set, along with the observations collected by one-shot knowledge gradient for maximal reliability (KG-MR) and the algorithm of Huang & Chan (2010). The optimal nominal design is shown by the pink dot, surrounded by an ellipse indicating one standard deviation of the normally distributed perturbation. The right panel shows the probability of failure over the domain, as defined in (2).

2. Problem Definition

Let $\mathcal{X} \subset \mathbb{R}^{d_x}$ and $\mathcal{Y} \subset \mathbb{R}^{d_y}$ and $\mathcal{U} \subset \mathbb{R}^{d_u}$ denote the spaces of the nominal design, perturbed design and perturbation variables. Let $f : \mathcal{Y} \rightarrow \mathbb{R}$ be a black-box function and suppose that we can make expensive observations $v = f(\mathbf{y})$ at points $\mathbf{y} \in \mathcal{Y}$ of our choice. Let \mathbf{u} be a random vector taking values in \mathcal{U} , and let $\mathbf{g} : \mathcal{X} \times \mathcal{U} \rightarrow \mathcal{Y}$ be a known function mapping pairs of nominal designs \mathbf{x} and perturbations \mathbf{u} to perturbed designs \mathbf{y} . Let $c \in \mathbb{R}$ be a threshold such that perturbed designs $\mathbf{y} \in \mathcal{Y}$ with $f(\mathbf{y}) \geq c$ are regarded as infeasible. Finally, let $\mathcal{Y}_{\text{feas}} \subset \mathcal{Y}$ be a subspace such that values $\mathbf{y} \in \mathcal{Y} \setminus \mathcal{Y}_{\text{feas}}$ are regarded as infeasible regardless of the value of $f(\mathbf{y})$. This includes simpler constraints on \mathbf{y} which are not a black-box, such as bound constraints on a normally perturbed nominal design. The problem tackled in this paper is to minimize the failure probability associated with the nominal design,

$$\min_{\mathbf{x} \in \mathcal{X}} P(\mathbf{x}) \quad (1a)$$

$$P(\mathbf{x}) := \mathbb{P}_{\mathbf{u}} \left(f \circ \mathbf{g}(\mathbf{x}, \mathbf{u}) \geq c \text{ or } \mathbf{g}(\mathbf{x}, \mathbf{u}) \notin \mathcal{Y}_{\text{feas}} \right). \quad (1b)$$

Here $f \circ \mathbf{g}(\mathbf{x}, \mathbf{u}) = f(\mathbf{g}(\mathbf{x}, \mathbf{u}))$ denotes function composition and $\mathbb{P}_{\mathbf{u}}$ denotes probability over $\mathbf{u} \sim \mathbb{P}_{\mathbf{u}}$.

The following lemma, which is proved in Appendix A, ensures that Problem (1) has at least one solution.

Lemma 2.1. *Suppose that $f : \mathcal{Y} \rightarrow \mathbb{R}$ is continuous, $\mathbf{g} : \mathcal{X} \times \mathcal{U} \rightarrow \mathcal{Y}$ is continuous and that the distribution of $\mathbb{P}_{\mathbf{u}}$ has no mass on the limit state surface or boundary of $\mathcal{Y}_{\text{feas}}$. Then the failure probability $P : \mathcal{X} \rightarrow [0, 1]$ is continuous. If also \mathcal{X} is compact then P attains its minimum value for some $\mathbf{x}^* \in \mathcal{X}$.*

In the experiments, we focus on the case where $d_x = d_y = d_u = d$, $\mathcal{X} = \mathcal{Y}_{\text{feas}} \subset \mathbb{R}^d$ is a hyper-rectangle, $\mathcal{Y} = \mathcal{U} = \mathbb{R}^d$ and $\mathbf{g}(\mathbf{x}, \mathbf{u}) = \mathbf{x} + \mathbf{u}$, but the core concepts are applicable in the general case. In this specific case, (1b) becomes

$$P(\mathbf{x}) = \mathbb{P}_{\mathbf{u}} \left(f(\mathbf{x} + \mathbf{u}) \geq c \text{ or } \mathbf{x} + \mathbf{u} \notin \mathcal{Y}_{\text{feas}} \right). \quad (2)$$

3. Related Work

BO has been previously applied in reliability-based design optimization (Dubourg et al., 2011; Janusevskis & Le Riche, 2013; El Amri et al., 2023; Pelamatti et al., 2023) in which the authors seek to minimize an objective in expectation subject to constraints which must hold with some high minimum probability. Tsai et al. (2023) solve a similar problem where the constraints must hold in expectation. In contrast, we consider the problem where the constraints are promoted to the place of the objective, and seek a solution which satisfies a constraint with maximal probability.

Quantile and worst-case optimization are also a closely related problems to which BO has been successfully applied (Cakmak et al., 2020; Nguyen et al., 2021; Picheny et al., 2022; ur Rehman et al., 2014; Han et al., 2025). However, here the risk level is fixed and the nominal design \mathbf{x} is chosen to give the best possible threshold c , while this paper concerns the reverse problem.

Related problems arise in active learning, including the estimation of the failure probability $\mathbb{P}(f(\mathbf{u}) \geq c)$ (called *reliability analysis*), and the estimation of particular level sets of a black-box function $\{\mathbf{u} \in \mathcal{U} : f(\mathbf{u}) = c\}$, the limit state surface being such a set. Works in this area include Picheny et al. (2010), Bichon et al. (2008), Bect et al. (2011), Knudde et al. (2019) and Booth & Renganathan (2025).

The first and second order reliability methods (FORM / SORM) (Hasofer & Lind, 1974; Breitung, 1984) capitalize on the uneven contribution of different parts of the limit state surface to the failure probability by replacing it with a local linear or quadratic approximation about the point on the limit state surface with highest probability density $p(\mathbf{u} | f(\mathbf{u}) = c)$. While this is an acceptable approximation for many estimation problems, in the optimization case the optimal nominal design \mathbf{x}^* will instead be trapped between $d + 1$ equally most-probable points – the minimum number of vertices for a polyhedron in \mathbb{R}^d . While an algorithm which attempts to track these points as the proposed nominal design converges is conceivable, it is not the approach we follow in this paper.

As noted in the introduction, we are particularly interested in the case where the failure probability is very small, which demands techniques from rare-event estimation such as importance sampling (Kloek & Van Dijk, 1978) or subset simulation (Au & Beck, 2001). Modern approaches to both these use Markov chain Monte Carlo (MCMC) (Papaioannou et al., 2015; Papakonstantinou et al., 2023; Tong & Stadler, 2023) and density estimation (De Boer et al., 2005; Kroese et al., 2013). Tabandeh et al. (2022) give a review of modern importance sampling methods. Importance sampling has been applied to the problem of reliability-based design optimization by Fonseca et al. (2006) in a manner agnostic to the presence of a surrogate model.

Among works which seek to maximize reliability, Wang et al. (2018) use BO to decide where to run an adaptive Monte Carlo estimate of the reliability, while Weller et al. (2022) propose a nested scheme using BO to train a Gaussian process which is accurate on the limit state surface then apply an evolutionary algorithm to select promising nominal designs. They require 10,000s and 1,000s of simulations respectively and assume that the simulations are sufficiently fast that this is feasible. To the best of our knowledge, two works exist which don't require so many simulations. Huang & Chan (2010) propose an algorithm which chooses between four different acquisition criteria to explore the limit state surface. Bichon et al. (2012) propose three extensions to their earlier work on efficient global reliability analysis (EGRA) to tackle various problems related to reliability-based design optimization, one of which is a constrained version of (1). These are used as baseline algorithms for the numerical comparison in Section 8.

4. Background

Bayesian Optimization (BO) is a sample-efficient, global optimization algorithm for black-box functions (Frazier, 2018; Garnett, 2023). A prior belief, typically a Gaussian process (GP), is placed on the objective and an acquisition strategy trades off between exploring regions with high un-

certainty and exploiting regions which are already expected to give good values. In the vanilla case, evaluations are made sequentially, where at each step the hyper-parameters of the probabilistic prior are fitted to the available data, then the acquisition strategy is used to give the next sample location, and finally the black-box function is evaluated at that location. The whole process is begun with an initial, space-filling design such as a Sobol' sample, and is typically run until an evaluation budget is exhausted.

Thompson sampling (TS) is one such acquisition strategy, where the next sample location is the maximum of a random sample from the posterior for the objective. Conversely, knowledge gradient (KG) (Frazier et al., 2009; Scott et al., 2011) is the one-step look-ahead Bayes-optimal policy when the final recommendation is the maximum of the posterior mean of the objective.

Importance Sampling is a variance reduction technique for Monte Carlo (MC) estimates of rare event probabilities (Tabandeh et al., 2022). For modest sample sizes, N_u , the standard MC estimate $P(\mathbf{x}) \approx \frac{1}{N} \sum_{i=1}^{N_u} \mathbb{I}_{\Omega_i}$ will likely observe no failures, where here we have written $\Omega_i = \{f \circ \mathbf{g}(\mathbf{x}, \mathbf{u}_i) \geq c \text{ or } \mathbf{g}(\mathbf{x}, \mathbf{u}_i) \notin \mathcal{Y}_{\text{feas}}\}$. Indeed, the standard deviation of this estimator is $\sqrt{P(\mathbf{x})(1 - P(\mathbf{x}))}/N_u$. If the true failure probability at the optimal \mathbf{x}^* is $P(\mathbf{x}^*) = 10^{-7}$ then to get the standard deviation of the estimator below 10% of the failure probability, we need $N_u \gtrsim 10^9$ samples.

Importance sampling reduces the variance by sampling from a distribution $\mathbb{Q}_{\mathbf{u}}$ under which failures occur more frequently, then reweighting samples to account for their true probabilities under $\mathbb{P}_{\mathbf{u}}$. Assuming that $\mathbb{P}_{\mathbf{u}}$ and $\mathbb{Q}_{\mathbf{u}}$ have densities denoted $p(\cdot)$ and $q(\cdot)$ respectively, the importance sampling estimate is $P(\mathbf{x}) \approx \frac{1}{N_u} \sum_{i=1}^{N_u} \frac{p(\mathbf{u}_i)}{q(\mathbf{u}_i)} \mathbb{I}_{\Omega_i}$. A simple choice for $\mathbb{Q}_{\mathbf{u}}$ is to use the same parametric family as $\mathbb{P}_{\mathbf{u}}$ with increased variance. For example, if $\mathbb{P}_{\mathbf{u}} = \mathcal{N}(0, \Sigma_u)$ then we choose $\mathbb{Q}_{\mathbf{u}} = \mathcal{N}(0, \tau^2 \Sigma_u)$.

5. Recommended Design

We begin by assuming that we have made a number of observations of the black-box function f and wish to extract a recommended nominal design. Problem (1) is one of partial or indirect information, where rather than observing the objective $P(\mathbf{x})$ we instead observe $f(\mathbf{y})$ at a finite set of \mathbf{y} . Therefore, we have never collected enough information to fully know $P(\mathbf{x})$ and must resort to a model.

Let us model the black-box objective $f : \mathcal{Y} \rightarrow \mathbb{R}$ using a GP prior, $f \sim \mathcal{GP}(\mu, k)$. To ensure the optimization problems are well defined, we assume that f is sample-continuous.

Given this prior belief, we use the posterior mean of the GP as a surrogate for f . Therefore, after n observations

$v_1 = f(\mathbf{y}_1), \dots, v_n = f(\mathbf{y}_n)$, the recommended nominal design is

$$\mathbf{x}_n^* \in \arg \min_{\mathbf{x} \in \mathcal{X}} P_n(\mathbf{x}) := \mathbb{E}[P(\mathbf{x}) \mid \mathcal{F}_n] \quad (3)$$

where \mathcal{F}_n is the sigma-algebra generated by the n observations and $P_n(\mathbf{x})$ is the expected failure probability. Lemma 5.1 establishes that the arg-min in (3) is non-empty.

The following lemma is proved in Appendix A.

Lemma 5.1. *Suppose that f is a sample-continuous Gaussian process and that $\mathbf{g} : \mathcal{X} \times \mathcal{U} \rightarrow \mathcal{Y}$ is continuous. Then under mild regularity conditions on $\mathbb{P}_{\mathbf{u}}$ made explicit in Appendix A, $P_n : \mathcal{X} \rightarrow [0, 1]$ is continuous. If also \mathcal{X} is compact then P_n attains its minimum value for some $\mathbf{x}_n^* \in \mathcal{X}$.*

Writing (1b) as an expectation over a combination of indicators and appealing to Fubini's theorem to switch the order of integration, we obtain

$$\begin{aligned} P_n(\mathbf{x}) &= \mathbb{E}[P(\mathbf{x}) \mid \mathcal{F}_n] \\ &= \mathbb{E}_{\mathbf{u}} \left[\mathbb{E}_{\mathbf{u}} \left[\mathbb{I}_{\{f \circ \mathbf{g}(\mathbf{x}, \mathbf{u}) \geq c\}} \mathbb{I}_{\{\mathbf{g}(\mathbf{x}, \mathbf{u}) \in \mathcal{Y}_{\text{feas}}\}} \right. \right. \\ &\quad \left. \left. + \mathbb{I}_{\{\mathbf{g}(\mathbf{x}, \mathbf{u}) \notin \mathcal{Y}_{\text{feas}}\}} \right] \mid \mathcal{F}_n \right] \\ &= \mathbb{E}_{\mathbf{u}} \left[\Phi_n(\mathbf{x}, \mathbf{u}; c) \mathbb{I}_{\{\mathbf{g}(\mathbf{x}, \mathbf{u}) \in \mathcal{Y}_{\text{feas}}\}} + \mathbb{I}_{\{\mathbf{g}(\mathbf{x}, \mathbf{u}) \notin \mathcal{Y}_{\text{feas}}\}} \right] \quad (4) \end{aligned}$$

where we write

$$\Phi_n(\mathbf{x}, \mathbf{u}; c) = \Phi \left(\frac{\mu_n(\mathbf{g}(\mathbf{x}, \mathbf{u})) - c}{\sqrt{k_n(\mathbf{g}(\mathbf{x}, \mathbf{u}), \mathbf{g}(\mathbf{x}, \mathbf{u}))}} \right) \quad (5)$$

and where μ_n and k_n are the posterior mean and covariance functions of f conditional on \mathcal{F}_n .

Finally, in the case of very small failure probabilities, we care more about the order of magnitude of the failure probability than the failure probability itself. Thus, we define

$$R_n(\mathbf{x}) = -\log P_n(\mathbf{x}). \quad (6)$$

The negative here simply converts from a minimization problem to a maximization problem. While R_n is maximized at the same place where P_n is minimized, taking the logarithm will be convenient since the default convergence tolerances for gradient-based optimizers will likely cause early termination for P_n but will remain applicable to R_n . Of course, $R_n(\mathbf{x})$ is only well defined if $P_n(\mathbf{x}) > 0$. However, if $P_n(\mathbf{x}) = 0$ then $P(\mathbf{x}) = 0$ almost surely and so \mathbf{x} is an optimal point with zero probability of failure and the optimization problem is solved. Therefore, we can safely ignore this case.

6. Acquisition Strategies

We now introduce the two acquisition strategies proposed in this paper.

6.1. Thompson Sampling for Maximizing Reliability (TS-MR)

The first algorithm we propose is based on Thompson sampling. At each stage of the optimization, we draw a random sample \tilde{f} from the GP posterior on f and use this to compute the nominal design with maximal reliability, \mathbf{x}_{n+1} .

$$\begin{aligned} \mathbf{x}_{n+1} &\in \\ &\arg \min_{\mathbf{x} \in \mathcal{X}} \mathbb{P}_{\mathbf{u}} \left(\tilde{f} \circ \mathbf{g}(\mathbf{x}, \mathbf{u}) \geq c \text{ or } \mathbf{g}(\mathbf{x}, \mathbf{u}) \notin \mathcal{Y}_{\text{feas}} \right). \quad (7) \end{aligned}$$

We then choose a perturbation \mathbf{u}_{n+1} which maximizes the product of the probability density of that perturbation and the variance of the failure indicator at that perturbation,

$$\mathbf{u}_{n+1} \in \arg \max_{\mathbf{u} \in \mathcal{U}_{\text{feas}}^{n+1}} \alpha_n^{\text{MV}}(\mathbf{u}; \mathbf{x}_{n+1}), \quad (8a)$$

$$\begin{aligned} \alpha_n^{\text{MV}}(\mathbf{u}; \mathbf{x}_{n+1}) &= p(\mathbf{u}) \text{Var}[\mathbb{I}_{\{f \circ \mathbf{g}(\mathbf{x}_{n+1}, \mathbf{u}) \geq c\}} \mid \mathcal{F}_n] \\ &= p(\mathbf{u}) \Phi_n(\mathbf{x}_{n+1}, \mathbf{u}; c) (1 - \Phi_n(\mathbf{x}_{n+1}, \mathbf{u}; c)). \quad (8b) \end{aligned}$$

For the combination to be feasible, the optimization is constrained to lie in $\mathcal{U}_{\text{feas}}^{n+1} = \mathbf{g}_{\mathbf{x}_{n+1}}^{-1}(\mathcal{Y}_{\text{feas}}) \subset \mathcal{U}$ where we have written $\mathbf{g}_{\mathbf{x}_{n+1}}(\cdot) = \mathbf{g}(\mathbf{x}_{n+1}, \cdot)$. The idea of α_n^{MV} is to encourage exploration of those parts of the limit state surface which are near to the proposed nominal design \mathbf{x}_{n+1} . Finally, the next sample location is given by

$$\mathbf{y}_{n+1} = \mathbf{g}(\mathbf{x}_{n+1}, \mathbf{u}_{n+1}). \quad (9)$$

6.2. Knowledge Gradient for Maximizing Reliability (KG-MR)

As noted in Section 5, the problem in (1) is one of partial or indirect information. KG has previously had much success being applied to such problems (Daulton et al., 2023; Buathong et al., 2024; Buckingham et al., 2025a;b).

KG applied to the value functions $(R_n)_{n \geq 1}$ defined in (6) is the change in expected value of the maximum of the negative log-failure probability before and after the next observation, conditional on that observation being made at the specified $\mathbf{y} \in \mathcal{Y}_{\text{feas}}$. That is, after n observations it is the function $\alpha_n^{\text{KG-MR}} : \mathcal{Y}_{\text{feas}} \rightarrow \mathbb{R}$ given by

$$\begin{aligned} \alpha_n^{\text{KG-MR}}(\mathbf{y}) &= \\ &\mathbb{E} \left[\max_{\mathbf{x} \in \mathcal{X}} R_{n+1}(\mathbf{x}) \mid \mathcal{F}_n, \mathbf{y}_{n+1} = \mathbf{y} \right] - \max_{\mathbf{x} \in \mathcal{X}} R_n(\mathbf{x}). \quad (10) \end{aligned}$$

It approximates the one-step look-ahead Bayes-optimal policy for minimizing the logarithm of the failure probability by replacing $P(\mathbf{x})$ with $P_n(\mathbf{x})$ in the expected utility $\mathbb{E}[-\log P(\mathbf{x}) \mid \mathcal{F}_n] \approx -\log P_n(\mathbf{x}) = R_n(\mathbf{x})$. This

greatly improves computational efficiency and similar plug-in approximations have previously performed well in multi-objective BO (Daulton et al., 2023).

Remark 6.1. As noted earlier, if $\max_{\mathbf{x} \in \mathcal{X}} R_{n+1}(\mathbf{x}) = \infty$ then we have found a point with almost surely zero probability of failure and so need not worry that $\alpha_n^{\text{KG-MR}}(\mathbf{y})$ is not well defined.

Remark 6.2. In the case where the optimal failure probability isn't as extreme, we could very well drop the logarithm and define it directly from P_n .

Lemma 6.3. *The KG-MR acquisition function in (10) is everywhere non-negative. That is,*

$$\forall n \geq 0 \quad \forall \mathbf{y} \in \mathcal{Y}_{\text{feas}} \quad \alpha_n^{\text{KG-MR}}(\mathbf{y}) \geq 0.$$

This is proved in Appendix A.

7. Approximations

In order to optimize to find recommendations in (3) or query points in (7), (8) and (10), we will need to approximate (4), (6) and the acquisition functions. A naive approximation for (4) uses an MC approximation over N_u independent points $\mathbf{u}_1, \dots, \mathbf{u}_{N_u} \sim \mathbb{P}_{\mathbf{u}}$,

$$\begin{aligned} P_n(\mathbf{x}) \approx \frac{1}{N_u} \sum_{i=1}^{N_u} \Phi_n(\mathbf{x}, \mathbf{u}_i; c) \mathbb{I}_{\{\mathbf{g}(\mathbf{x}, \mathbf{u}_i) \in \mathcal{Y}_{\text{feas}}\}} \\ + \mathbb{I}_{\{\mathbf{g}(\mathbf{x}, \mathbf{u}_i) \notin \mathcal{Y}_{\text{feas}}\}}. \end{aligned} \quad (11)$$

However, there are two problems with optimizing this approximation directly. Firstly, while we were able to get rid of the indicator $\mathbb{I}_{\{f \circ g(\mathbf{x}, \mathbf{u}) \geq c\}}$ analytically thanks to the uncertainty in the GP, we could not remove all the indicators and the remaining ones mean the approximation in (11) is not continuous in \mathbf{x} . Secondly, if the optimal failure probability is rare, then it is likely that all of the \mathbf{u}_i will lie well below the failure threshold, meaning $\Phi_n(\mathbf{x}, \mathbf{u}_i; c) \approx 0$ has almost zero gradient and we will have no gradient information to use to optimize $P_n(\mathbf{x})$.

To address the first of these issues, we use an ad-hoc smoothing of the indicator function, described in Appendix D.1. Specifically, we approximate $\mathbb{I}_{\{\mathbf{g}(\mathbf{x}, \mathbf{u}) \in \mathcal{Y}_{\text{feas}}\}} \approx \iota(\mathbf{g}(\mathbf{x}, \mathbf{u}); \delta)$, where δ determines the width of the smoothed region around the boundary $\partial \mathcal{Y}_{\text{feas}}$. In practice, we find a very small amount of smoothing to be sufficient and set $\delta = \min(0.05\ell_{\min}, 0.1)$ where ℓ_{\min} is the smallest sidelength of $\mathcal{Y}_{\text{feas}}$.

For the second issue, caused by near zero contributions to the failure probability, we use importance sampling with sampling distribution $\mathbb{Q}_{\mathbf{u}} = \mathcal{N}(0, \tau^2 \Sigma_u)$. In practice, we find a value of $\tau = 3$ works well with optimal failure probabilities in the range $10^{-6} - 10^{-8}$.

7.1. Approximation for Recommendations

Introducing the indicator smoothing approximations and importance sampling into (3) gives the following estimates for $P_n(\mathbf{x})$, $R_n(\mathbf{x})$ and the recommendation \mathbf{x}_n^* ,

$$\hat{\mathbf{x}}_n^* \in \arg \max_{\mathbf{x} \in \mathcal{X}} \hat{R}_n(\mathbf{x}) = \arg \min_{\mathbf{x} \in \mathcal{X}} \hat{P}_n(\mathbf{x}), \quad (12a)$$

$$\hat{R}_n(\mathbf{x}) = -\log \hat{P}_n(\mathbf{x}), \quad (12b)$$

$$\hat{P}_n(\mathbf{x}) = \frac{1}{N_u} \sum_{i=1}^{N_u} \frac{p(\mathbf{u}_i)}{q(\mathbf{u}_i)} \hat{J}_n(\mathbf{x}, \mathbf{u}_i), \quad (12c)$$

$$\begin{aligned} \hat{J}_n(\mathbf{x}, \mathbf{u}) = \Phi_n(\mathbf{x}, \mathbf{u}; c) \iota(\mathbf{g}(\mathbf{x}, \mathbf{u}); \delta) \\ + (1 - \iota(\mathbf{g}(\mathbf{x}, \mathbf{u}); \delta)). \end{aligned} \quad (12d)$$

We solve (12a) via multi-start L-BFGS-B, a deterministic gradient-based optimizer (see Appendix D.3).

Further, it is known that quasi-Monte Carlo (qMC) improves the convergence rate of MC estimates from $\mathcal{O}(1/\sqrt{N_u})$ to $\mathcal{O}((\log N_u)^{d_u}/N_u)$ for many integrands (Lemieux, 2009). Where the distribution $\mathbb{P}_{\mathbf{u}}$ is amenable, we use a qMC approximation for (12c) using a Sobol' sample in place of independent samples. This is possible for Gaussian and uniformly distributed \mathbf{u} .

7.2. Approximation for Thompson Sampling

The first approximation required in TS-MR is to draw the sample \tilde{f} conditional on \mathcal{F}_n . For this, we use the pathwise sampling method of Wilson et al. (2020; 2021) with $N_{\text{rff}} = 1024$ random Fourier features (RFFs). We use the following approximation, analogous to (12), using $\tilde{P}(\mathbf{x})$ to denote the failure probability in (7) obtained using \tilde{f} ,

$$\tilde{P}(\mathbf{x}) \approx \frac{1}{N_u} \sum_{i=1}^{N_u} \frac{p(\mathbf{u}_i)}{q(\mathbf{u}_i)} \tilde{J}(\mathbf{x}, \mathbf{u}_i) \quad (13a)$$

$$\begin{aligned} \tilde{J}(\mathbf{x}, \mathbf{u}) \approx \Phi \left(\frac{\tilde{f} \circ \mathbf{g}(\mathbf{x}, \mathbf{u}) - c}{\rho} \right) \iota(\mathbf{g}(\mathbf{x}, \mathbf{u}); \delta) \\ + (1 - \iota(\mathbf{g}(\mathbf{x}, \mathbf{u}); \delta)). \end{aligned} \quad (13b)$$

Here we have mimicked the smoothing of $\mathbb{I}_{\{\tilde{f} \circ g(\mathbf{x}, \mathbf{u}) \geq c\}}$ in (12d) using a parameter $\rho > 0$. Again, we optimize this approximation of $\tilde{P}(\mathbf{x})$ using multi-start L-BFGS-B, performed in log-space. The second stage of TS-MR requires optimizing α_n^{MV} in (8). This requires neither importance sampling nor indicator smoothing. However, we do perform it in log-space, using the `log_ndtr()` function in PyTorch to compute $\log \Phi_n(\mathbf{x}_{n+1}, \mathbf{u}; c)$ and $\log(1 - \Phi_n(\mathbf{x}_{n+1}, \mathbf{u}; c))$ in a numerically stable manner. The full algorithm is presented in Algorithm 1.

Algorithm 1 Thompson Sampling for Maximal Reliability

Input: Initial sample size n_0 , evaluation budget n_{tot} , qMC sample size N_u , number of Fourier features N_{rff} , smoothing parameters ρ, δ

- 1: Evaluate f at n_0 points, chosen according to a scrambled Sobol' sequence on $\mathcal{Y}_{\text{feas}}$
- 2: **for** $n = n_0, \dots, n_{\text{tot}} - 1$ **do**
- 3: Fit MAP hyperparameters of GP prior on f
- 4: Sample RFF features and weights for $\tilde{f} \sim \mathcal{GP}(\mu_n, k_n)$
- 5: Generate qMC sample $(\mathbf{u}_1, \dots, \mathbf{u}_{N_u}) \sim \mathbb{Q}_{\mathbf{u}}$
- 6: Optimize $\mathbf{x}_{n+1} \leftarrow \arg \min_{\mathbf{x} \in \mathcal{X}} \log \tilde{P}(\mathbf{x})$ using the approximation in (13)
- 7: Optimize α_n^{MV} defined in (8) to give $\mathbf{u}_{n+1} \leftarrow \arg \max_{\mathbf{u} \in \mathcal{U}_{\text{feas}}^{n+1}} \log \alpha_n^{\text{MV}}(\mathbf{u}; \mathbf{x}_{n+1})$
- 8: Set $\mathbf{y}_{n+1} \leftarrow \mathbf{g}(\mathbf{x}_{n+1}, \mathbf{u}_{n+1})$
- 9: Evaluate expensive function, $f(\mathbf{y}_{n+1})$
- 10: **end for**
- 11: Compute recommendation $\hat{\mathbf{x}}_{n_{\text{tot}}}^*$ using (12)

7.3. Approximations for Knowledge Gradient

The ‘one-shot’ approximation for KG (Balandat et al., 2020) uses an MC or qMC estimate over N_v fantasy observations for the expectation over the next observation v_{n+1} in (10). Variables from the maximization for each element of the MC sum are pulled out to the front to create a single, high-dimensional optimization problem,

$$\max_{\mathbf{y} \in \mathcal{Y}_{\text{feas}}} \hat{\alpha}_n(\mathbf{y}) = \max_{\mathbf{y} \in \mathcal{Y}_{\text{feas}}, \mathbf{x}_1, \dots, \mathbf{x}_{N_v} \in \mathcal{X}} \frac{1}{N_v} \sum_{i=1}^{N_v} \hat{R}_{n+1}(\mathbf{x}_i; \mathbf{y}, z_i) - \max_{\mathbf{x} \in \mathcal{X}} \hat{R}_n(\mathbf{x}). \quad (14)$$

Here $\hat{R}_n(\mathbf{x})$ is as in (12b) and $\hat{R}_{n+1}(\mathbf{x}; \mathbf{y}, z)$ is the same but assuming the $(n+1)$ -th observation of f is at \mathbf{y} with value $v = f(\mathbf{y}) = \mu_n(\mathbf{y}) + z\sqrt{k_n(\mathbf{y}, \mathbf{y})}$. This use of the reparametrization trick separates the randomness and the dependence on \mathbf{y} . The sample z_1, \dots, z_{N_v} is a sample of N_v standard Gaussian variables. If they are independent then this is a standard MC estimate, however in practice we use a Sobol' sample passed through a Box-Muller transform to give a qMC estimate as is standard in BoTorch (Balandat et al., 2020). The dimension of the optimization problem in (14) is $d_y + N_v d_x$.

An alternative which avoids the high-dimensional optimization in (14) is to replace the maximization over $\mathbf{x} \in \mathcal{X}$ in (10) by maximization over a finite set $\mathcal{X}_{\text{disc}} \subset \mathcal{X}$ sampled from a scrambled Sobol' sequence or other space-filling design (e.g. Buathong et al., 2024; Buckingham et al., 2025a). Combining this with the (q)MC estimate for the expectation

Algorithm 2 Knowledge Gradient for Maximal Reliability

Input: Initial sample size n_0 , evaluation budget n_{tot} , qMC sample sizes N_u, N_v ; for discrete KG-MR the discretization size N_x ; for one-shot KG-MR the smoothing parameter δ

- 1: Evaluate f at n_0 points, chosen according to a scrambled Sobol' sequence on $\mathcal{Y}_{\text{feas}}$
- 2: **for** $n = n_0, \dots, n_{\text{tot}} - 1$ **do**
- 3: Fit MAP hyperparameters of GP prior on f
- 4: Generate qMC samples $(\mathbf{u}_1, \dots, \mathbf{u}_{N_u}) \sim \mathbb{Q}_{\mathbf{u}}$ and $(z_1, \dots, z_{N_v}) \sim \mathcal{N}(0, 1)$
- 5: If using discrete KG-MR, sample $\mathcal{X}_{\text{disc}}$ of size N_x using a scrambled Sobol' sequence
- 6: Optimize $\mathbf{y}_{n+1} \leftarrow \arg \max_{\mathbf{y} \in \mathcal{Y}_{\text{feas}}} \hat{\alpha}_n(\mathbf{y})$ using either (15) or (14)
- 7: Evaluate expensive function, $f(\mathbf{y}_{n+1})$
- 8: **end for**
- 9: Compute recommendation $\hat{\mathbf{x}}_{n_{\text{tot}}}^*$ using (12)

over v_{n+1} gives

$$\hat{\alpha}_n(\mathbf{y}) = \frac{1}{N_v} \sum_{i=1}^{N_v} \max_{\mathbf{x} \in \mathcal{X}_{\text{disc}}} \hat{R}_{n+1}(\mathbf{x}; \mathbf{y}, z_i) - \max_{\mathbf{x} \in \mathcal{X}_{\text{disc}}} \hat{R}_n(\mathbf{x}). \quad (15)$$

This approximation is generally accurate when d_x is small, but suffers from the curse of dimensionality for larger d_x .

For the discrete approximation in (15), the set $\mathcal{X}_{\text{disc}}$ is fixed so we do not need to worry about differentiability of \hat{R}_n and \hat{R}_{n+1} with respect to \mathbf{x} and can set the bounds smoothing factor $\delta = 0$. For the one-shot approximation in (14), we keep $\delta = \min(0.05\ell_{\min}, 0.1)$.

Both approximations are optimized using multi-start L-BFGS-B, paying particular care to the initial points used for the one-shot approximation (see Appendix B). The full algorithm is summarized in Algorithm 2.

8. Experiments

In order to judge how well the TS-MR and two KG-MR approximations perform, they are compared to two algorithms which are already present in the literature: the algorithm of Huang & Chan (2010) (denoted HC) and efficient global reliability analysis (EGRA) proposed by Bichon et al. (2008; 2012). These methods are outlined in Appendix C and parameter choices are detailed in Appendix D.5. Additionally, a comparison with two simpler baseline algorithms is made. The first is a random sampling approach which selects points $\mathbf{y}_1, \mathbf{y}_2, \dots$ according to a scrambled Sobol' sequence, and the second uses expected improvement (EI) to search for $\min_{\mathbf{y}} f(\mathbf{y})$ rather than minimizing the failure probability. For all methods compared, the same procedure is used for generating recommendations. That is, we optimize (12a)

with multi-start L-BFGS-B as described in Appendix D.3.

We compare the algorithms on three random problems sampled from a GP and nine frequently-used synthetic test problems, ranging from two to sixteen input dimensions. The problems all have $\mathcal{X} = \mathcal{Y} = \mathcal{U}$ and $g(\mathbf{x}, \mathbf{u}) = \mathbf{x} + \mathbf{u}$ to represent a perturbation about a nominal design. The perturbations used are normally distributed, $\mathbf{u} \sim \mathcal{N}(0, \Sigma_u)$, with diagonal covariance matrices Σ_u varying between problems.

Each algorithm is run 30 times on each test problem with a different random seed. For each repeat, a different initial design is randomly selected using a scrambled Sobol' sample with size depending on the problem dimension and specified in Appendix D.5. For all algorithms, the GP surrogate has a Matérn-5/2 kernel with MAP-estimated hyperparameters fitted as described in Appendix D.2.

8.1. Evaluation of the Recommendations

Given a recommended nominal design \mathbf{x}_n^* , we evaluate it using a qMC approximation of $P(\mathbf{x}_n^*)$ with importance sampling, and using the true test function,

$$P(\mathbf{x}_n^*) \approx \frac{1}{N_u} \sum_{i=1}^{N_u} \frac{p(\mathbf{u}_i)}{q(\mathbf{u}_i)} \left(\mathbb{I}_{\{f \circ g(\mathbf{x}_n^*, \mathbf{u}_i) \geq c\}} \mathbb{I}_{\{g(\mathbf{x}_n^*, \mathbf{u}_i) \in \mathcal{Y}_{\text{feas}}\}} + \mathbb{I}_{\{g(\mathbf{x}_n^*, \mathbf{u}_i) \notin \mathcal{Y}_{\text{feas}}\}} \right). \quad (16)$$

For this, we use $N_u = 2^{20} \approx 1,000,000$, which is larger than the values we used for either the acquisition function or for generating the recommendation. The same inflation method and scale factor for the importance sampling are used for this estimate as were used in the acquisition function and to generate recommendations. Since in all cases $\mathbb{Q}_{\mathbf{u}}$ is Gaussian, the qMC approximation uses a d -dimensional Sobol' sample with coordinates passed pairwise through a Box-Muller transform.

8.2. Results

Figure 1 shows an example of the samples made by the one-shot KG-MR and HC algorithms on the Styblinski-Tang (2D) test problem. Both algorithms mainly collect samples near to the limit state surface. However, KG-MR focuses its samples on the parts of the limit state surface which contribute to the failure probability at the optimal design, while HC spreads its samples evenly around the whole limit state surface. This is particularly a problem when the limit state surface intersects the problem boundary (see Appendix E).

Figure 2 shows the median failure probability and interquartile range for the recommended design at each point during the BO procedure. The first column contains the three GP

generated problems and the remainder contain the common synthetic problems with the potential for model-mismatch. The problems in the middle two columns were chosen to have an interesting limit state surface, while the problems in the last column are chosen to exhibit cases where KG-MR and TS-MR are not expected to outperform HC and EGRA.

One-shot KG-MR (osKG-MR) performs best or joint best in 10 of the 12 problems, and discrete KG-MR (dKG-MR) matches its performance in lower dimensions. In 10+ dimensions, the approximations in dKG-MR are too crude and slow the convergence. TS-MR also performs strongly, though it lags in the 2D GP, 16D GP, Branin and uncropped 10D Styblinski-Tang problems. HC and EGRA generally perform poorly in the 2D problems because they fail to focus on the relevant parts of the limit state surface (e.g. Figure 1 and Appendix E). In higher dimensions, they perform poorly on the GP problems but ok on the synthetic examples.

The problems in the last column of Figure 2 were chosen to exhibit cases where the KG-MR and TS-MR algorithms should not have an advantage. The 2D quadratic function has a circular limit state surface, meaning all parts of the limit state surface are equally important. Consequently, the HC algorithm matches the performance of KG-MR and TS-MR, while EGRA is not too far behind. Similarly, for the 6D Hartmann problem, the higher threshold pushes the limit state surface further towards the edges of the domain and the HC algorithm becomes competitive, although in this case EGRA performs similarly to Sobol' search. Finally, the HC and EGRA algorithms perform empirically well on the uncropped 10D Styblinski-Tang problem, with EGRA marginally beating HC and osKG-MR. This problem is highly multimodal, with 1024 local minima, of which 848 are feasible. We hypothesize that HC and EGRA have good local search properties, focusing on learning about the limit state surface around one of the good local minima found in the initial design. They are also computationally cheaper than osKG-MR (see Appendix F). Thompson sampling is known to over-explore in higher dimensions (Papenmeier et al., 2025), and makes no progress on this problem, while dKG-MR makes no progress because the approximating set is not able to capture enough of the problem's structure.

Similar conclusions hold in the case of non-extreme failure probabilities, where the importance sampling is not needed and the logarithms in KG-MR are dropped (see Appendix G). Notable differences include osKG-MR being the top or joint-top performer in all problems while TS-MR, HC and EGRA show improvements in some problems. Generally all algorithms converge faster. A sensitivity study in Appendix H shows that the KG-MR methods are fairly robust to the choice of the parameters N_u and N_v , but that the size of the discretization $N_x = |\mathcal{X}_{\text{disc}}|$ matters in higher dimensions for dKG-MR.

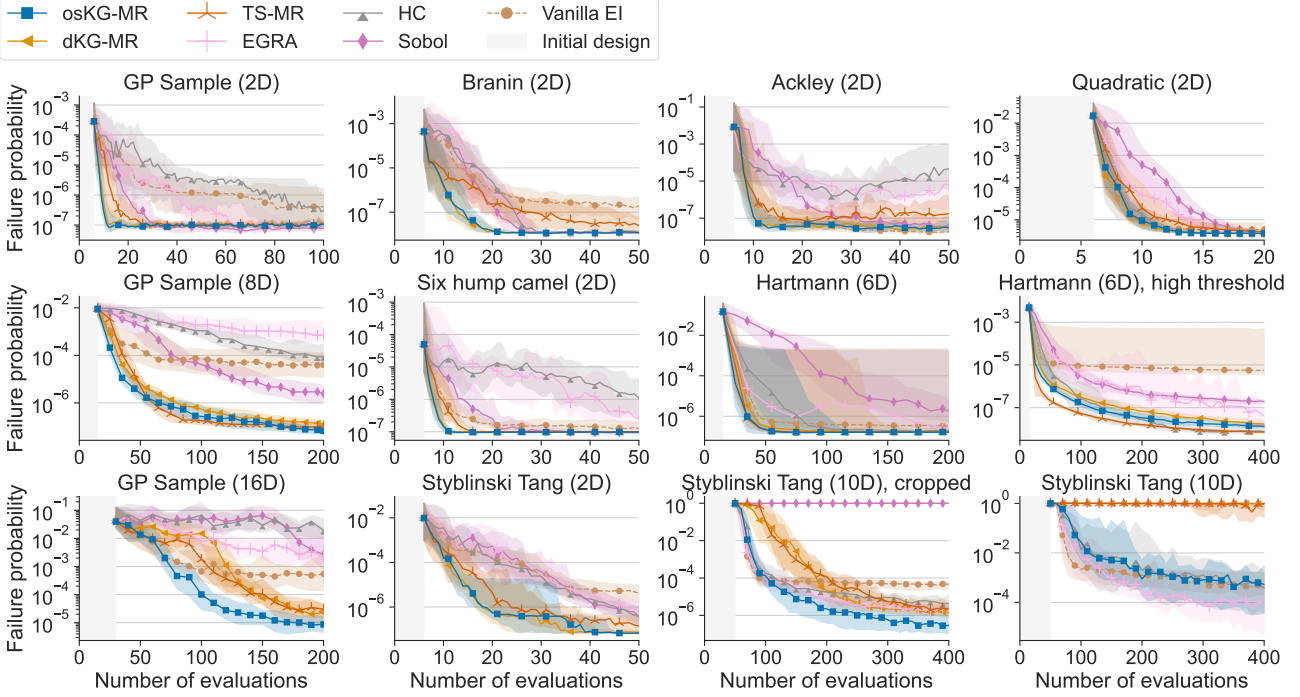


Figure 2. Failure probabilities for the 12 test problems. The first column contains the GP test problems, while the remaining columns are problems with potential for model mismatch. The last column contains problems for which KG-MR is not expected to have an advantage. The failure probability associated with the recommended solution is shown as a function of number of evaluations of the expensive black-box function. The solid lines show the median failure probability over 30 repeats and the shaded regions show the upper and lower quartiles.

9. Conclusions

This paper has introduced two distinct BO strategies targeting the equivalent problems of maximizing reliability, minimizing failure probability and maximizing yield. Approximations incorporating quasi-Monte Carlo and importance sampling have been proposed and experiments have been conducted on a range of synthetic problems both with and without model mismatch. On the 2D test problems, the KG-MR approaches perform equally well and converge faster than any of the alternatives. On the higher-dimensional problems, the approximations in the discrete KG-MR acquisition function are too coarse and harm the convergence, but the one-shot KG-MR remains the top performer, sometimes jointly with TS-MR. In all cases, the parameters of the KG-MR are very easy to tune, with the only choice to be made being how to split the computation budget between increasing N_u and N_v for osKG-MR in higher dimensions. The KG-MR algorithms are generally more expensive than the alternatives, in the slowest case taking of the order of 30-40 seconds to optimize using a GPU (see Appendix F). In summary, it should be recommended to use one-shot KG-MR unless the computation cost ceases to be negligible compared with the cost of evaluating f , in which case TS-MR is a fast alternative.

The algorithm of Huang & Chan (2010) is designed to tackle problems with multiple limit state functions f , which we haven't addressed empirically in this paper. However, the framework extends very naturally to this case making it a good avenue for future research. Similarly, constrained versions of the problem such as those tested on in Bichon et al. (2012) could be tackled. Additionally, the framework allows for any combination of the nominal design \boldsymbol{x} and perturbation \boldsymbol{u} , and this could be tested experimentally, for example with multiplicative perturbations as has been done in other related works (Cakmak et al., 2020; Daulton et al., 2022). Finally, adaptive importance sampling using kernel density estimation or MCMC could improve efficiency by ensuring all MC points for the estimation of $\mathbb{E}_{\boldsymbol{u}}$ are near to the limit state surface.

Acknowledgments

The authors would like to thank Tobias Grafke for an insightful discussion on rare event modeling. The first author was supported by the Engineering and Physical Sciences Research Council through the Mathematics of Systems II Centre for Doctoral Training at the University of Warwick (reference EP/S022244/1). The second author was supported by the Flemish Government under the Flanders Artificial

Intelligence Research program. Computing facilities were provided by the Scientific Computing Research Technology Platform of the University of Warwick.

Data Access Statement

This work is entirely theoretical, there is no data underpinning this publication.

Impact Statement

This paper presents work whose goal is to advance the field of Machine Learning. There are many potential societal consequences of our work, none which we feel must be specifically highlighted here.

References

Au, S.-K. and Beck, J. L. Estimation of small failure probabilities in high dimensions by subset simulation. *Probabilistic Engineering Mechanics*, 16(4):263–277, 2001. ISSN 0266-8920. URL [https://doi.org/10.1016/S0266-8920\(01\)00019-4](https://doi.org/10.1016/S0266-8920(01)00019-4).

Balandat, M., Karrer, B., Jiang, D., Daulton, S., Letham, B., Wilson, A. G., and Bakshy, E. Botorch: A framework for efficient monte-carlo Bayesian optimization. In Larochelle, H., Ranzato, M., Hadsell, R., Balcan, M., and Lin, H. (eds.), *Advances in Neural Information Processing Systems*, volume 33, pp. 21524–21538. Curran Associates, Inc., 2020. URL <https://proceedings.neurips.cc/paper/2020/file/f5b1b89d98b7286673128a5fb112cb9a-Paper.pdf>.

Bect, J., Ginsbourger, D., Li, L., Picheny, V., and Vazquez, E. Sequential design of computer experiments for the estimation of a probability of failure. *Statistics and Computing*, 22(3):773–793, 2011. ISSN 1573-1375. URL <https://doi.org/10.1007/s11222-011-9241-4>.

Betlei, A., Vladimirova, M., Sebbar, M., Urien, N., Rahier, T., and Heymann, B. Maximizing the success probability of policy allocations in online systems. *Proceedings of the AAAI Conference on Artificial Intelligence*, 38(10):11061–11068, 2024. ISSN 2374-3468. URL <https://doi.org/10.1609/aaai.v38i10.28982>.

Bichon, B. J., Eldred, M. S., Swiler, L. P., Mahadevan, S., and McFarland, J. M. Efficient global reliability analysis for nonlinear implicit performance functions. *AIAA Journal*, 46(10):2459–2468, 2008. ISSN 0001-1452. URL <https://doi.org/10.2514/1.34321>.

Bichon, B. J., Eldred, M. S., Mahadevan, S., and McFarland, J. M. Efficient global surrogate modeling for reliability-based design optimization. *Journal of Mechanical Design*, 135(011009), 2012. ISSN 1050-0472. URL <https://doi.org/10.1115/1.4022999>.

de Boer, P.-T., Kroese, D. P., Mannor, S., and Rubinstein, R. Y. A tutorial on the cross-entropy method. *Annals of Operations Research*, 134(1):19–67, 2005. ISSN 1572-9338. URL <https://doi.org/10.1007/s10479-005-5724-z>.

Booth, A. S. and Renganathan, S. A. Two-stage design for failure probability estimation with Gaussian process surrogates. *Journal of Quality Technology*, 57(5):500–516, October 2025. URL <https://doi.org/10.1080/00224065.2025.2562868>.

Breitung, K. Asymptotic approximations for multi-normal integrals. *Journal of Engineering Mechanics*, 110(3):357–366, 1984. ISSN 0733-9399. URL [https://doi.org/10.1061/\(ASCE\)0733-9399\(1984\)110:3\(357\)](https://doi.org/10.1061/(ASCE)0733-9399(1984)110:3(357)).

Buathong, P., Wan, J., Astudillo, R., Daulton, S., Balandat, M., and Frazier, P. I. Bayesian optimization of function networks with partial evaluations. In Salakhutdinov, R., Kolter, Z., Heller, K., Weller, A., Oliver, N., Scarlett, J., and Berkenkamp, F. (eds.), *International Conference on Machine Learning*, volume 235 of *Proceedings of Machine Learning Research*, pp. 4752–4784. PMLR, July 2024. URL <https://proceedings.mlr.press/v235/buathong24a.html>.

Buckingham, J. M., Couckuyt, I., and Branke, J. Bayesian optimization for non-convex two-stage stochastic optimization problems. *arXiv preprint*, February 2025a. URL <https://arxiv.org/abs/2408.17387>.

Buckingham, J. M., Rojas Gonzalez, S., and Branke, J. Knowledge gradient for multi-objective Bayesian optimization with decoupled evaluations. In Singh, H., Ray, T., Knowles, J., Li, X., Branke, J., Wang, B., and Oyama, A. (eds.), *Evolutionary Multi-Criterion Optimization*, volume 15513 of *Lecture Notes in Computer Science*, pp. 117–132, Singapore, February 2025b. Springer Nature Singapore. ISBN 978-981-96-3538-2. URL https://doi.org/10.1007/978-981-96-3538-2_9.

Cakmak, S., Astudillo Marban, R., Frazier, P. I., and Zhou, E. Bayesian optimization of risk measures. In *Advances in Neural Information Processing Systems*, volume 33, pp. 20130–20141. Curran Associates, Inc., 2020. URL https://proceedings.neurips.cc/paper_files/paper/2020/file/e8f2779682fd11fa2067beffc27a9192-Paper.pdf.

Charnes, A. and Cooper, W. W. Deterministic equivalents for optimizing and satisficing under chance constraints. *Operations Research*, 11(1):18–39, 1963. ISSN 0030-364X. URL <https://doi.org/10.1287/opre.11.1.18>.

Daulton, S., Cakmak, S., Balandat, M., Osborne, M. A., Zhou, E., and Bakshy, E. Robust multi-objective Bayesian optimization under input noise. In Chaudhuri, K., Jegelka, S., Song, L., Szepesvari, C., Niu, G., and Sabato, S. (eds.), *International Conference on Machine Learning*, volume 162 of *Proceedings of Machine Learning Research*, pp. 4831–4866. PMLR, July 2022. URL <https://proceedings.mlr.press/v162/daulton22a.html>.

Daulton, S., Balandat, M., and Bakshy, E. Hypervolume knowledge gradient: A lookahead approach for multi-objective Bayesian optimization with partial information. In *Proceedings of the 40th International Conference on Machine Learning*, volume 202 of *Proceedings of Machine Learning Research*, pp. 7167–7204. PMLR, July 2023. URL <https://proceedings.mlr.press/v202/daulton23a.html>.

Dubourg, V., Sudret, B., and Bourinet, J.-M. Reliability-based design optimization using kriging surrogates and subset simulation. *Structural and Multidisciplinary Optimization*, 44(5):673–690, 2011. ISSN 1615-1488. URL <https://doi.org/10.1007/s00158-011-0653-8>.

Durham, S., Flournoy, N., and Li, W. A sequential design for maximizing the probability of a favourable response. *Canadian Journal of Statistics*, 26(3):479–495, 1998. ISSN 1708-945X. URL <https://doi.org/10.2307/3315771>.

El Amri, R., Le Riche, R., Helbert, C., Blanchet-Scalliet, C., and Da Veiga, S. A sampling criterion for constrained bayesian optimization with uncertainties. *The SMAI Journal of computational mathematics*, 9:285–309, 2023. ISSN 2426-8399. URL <https://doi.org/10.5802/smai-jcm.102>.

Fonseca, J. R., Friswell, M. I., and Lees, A. W. Efficient robust design via Monte Carlo sample reweighting. *International Journal for Numerical Methods in Engineering*, 69(11):2279–2301, 2006. ISSN 1097-0207. URL <https://doi.org/10.1002/nme.1850>.

Frazier, P. I. Bayesian optimization. In *Recent Advances in Optimization and Modeling of Contemporary Problems*, pp. 255–278. INFORMS, October 2018. URL <https://doi.org/10.1287/educ.2018.0188>.

Frazier, P. I., Powell, W. B., and Dayanik, S. The knowledge-gradient policy for correlated normal beliefs. *INFORMS Journal on Computing*, 21:599–613, November 2009. ISSN 1091-9856. URL <https://doi.org/10.1287/ijoc.1080.0314>.

Gablonsky, J. and Kelley, C. A locally-biased form of the DIRECT algorithm. *Journal of Global Optimization*, 21(1):27–37, 2001. ISSN 1573-2916. URL <https://doi.org/10.1023/A:1017930332101>.

Garnett, R. *Bayesian optimization*. Cambridge University Press, 2023. ISBN 9781108425780. URL <https://bayesoptbook.com/>.

Han, J., Zheng, Y., Wang, K., Yang, C., and Yuan, X. Worst-case robust optimization based on an adaptive incremental Kriging metamodel. *Expert Systems with Applications*, 260:125372, January 2025. ISSN 0957-4174. URL <https://doi.org/10.1016/j.eswa.2024.125372>.

Hasofer, A. M. and Lind, N. C. Exact and invariant second-moment code format. *Journal of the Engineering Mechanics Division*, 100(1):111–121, 1974. URL <https://doi.org/10.1061/JMCEA3.0001848>.

Huang, Y.-C. and Chan, K.-Y. A modified efficient global optimization algorithm for maximal reliability in a probabilistic constrained space. *Journal of Mechanical Design*, 132(61002), 2010. ISSN 1050-0472. URL <https://doi.org/10.1115/1.4001532>.

Janusevskis, J. and Le Riche, R. Simultaneous kriging-based estimation and optimization of mean response. *Journal of Global Optimization*, 55(2):313–336, 2013. ISSN 1573-2916. URL <https://doi.org/10.1007/s10898-011-9836-5>.

Jones, D. R., Perttunen, C. D., and Stuckman, B. E. Lipschitzian optimization without the Lipschitz constant. *Journal of Optimization Theory and Applications*, 79(1):157–181, 1993. ISSN 1573-2878. URL <https://doi.org/10.1007/BF00941892>.

Jones, D. R., Schonlau, M., and Welch, W. J. Efficient global optimization of expensive black-box functions. *Journal of Global Optimization*, 13:455–492, December 1998. ISSN 09255001. URL <https://doi.org/10.1023/A:1008306431147>.

Kloek, T. and van Dijk, H. K. Bayesian estimates of equation system parameters: An application of integration by Monte Carlo. *Econometrica*, 46(1):1–19, 1978. ISSN 0012-9682. URL <https://doi.org/10.2307/1913641>.

Knudde, N., Couckuyt, I., Shintani, K., and Dhaene, T. Active learning for feasible region discovery. In *2019 18th IEEE International Conference On Machine Learning And Applications (ICMLA)*, pp. 567–572, 2019. URL <https://doi.org/10.1109/ICMLA.2019.00106>.

Kroese, D. P., Rubinstein, R. Y., and Glynn, P. W. Chapter 2 - the cross-entropy method for estimation. In Rao, C. R. and Govindaraju, V. (eds.), *Handbook of Statistics*, volume 31 of *Handbook of Statistics*, pp. 19–34. Elsevier, 2013. URL <https://doi.org/10.1016/B978-0-444-53859-8.00002-3>.

Lemieux. *Monte Carlo and Quasi-Monte Carlo Sampling*. Springer Series in Statistics. Springer, 1 edition, 2009. ISBN 978-0-387-78164-8 978-0-387-78165-5. URL <https://doi.org/10.1007/978-0-387-78165-5>.

Nguyen, Q. P., Dai, Z., Low, B. K. H., and Jaillet, P. Value-at-risk optimization with Gaussian processes. In *Proceedings of the 38th International Conference on Machine Learning*, pp. 8063–8072. PMLR, July 2021. URL <https://proceedings.mlr.press/v139/nguyen21b.html>.

Papaioannou, I., Betz, W., Zwiglmaier, K., and Straub, D. MCMC algorithms for subset simulation. *Probabilistic Engineering Mechanics*, 41:89–103, 2015. ISSN 0266-8920. URL <https://doi.org/10.1016/j.probengmech.2015.06.006>.

Papakonstantinou, K. G., Nikbakht, H., and Eshra, E. Hamiltonian MCMC methods for estimating rare events probabilities in high-dimensional problems. *Probabilistic Engineering Mechanics*, 74:103485, 2023. ISSN 0266-8920. URL <https://doi.org/10.1016/j.probengmech.2023.103485>.

Papenmeier, L., Cheng, N., Becker, S., and Nardi, L. Exploring exploration in Bayesian optimization. In *Proceedings of the Forty-first Conference on Uncertainty in Artificial Intelligence*, pp. 3388–3415. PMLR, July 2025. URL <https://proceedings.mlr.press/v286/papenmeier25a.html>.

Pelamatti, J., Le Riche, R., Helbert, C., and Blanchet-Scalliet, C. Coupling and selecting constraints in Bayesian optimization under uncertainties. *Optimization and Engineering*, 25(1):373–412, 2023. ISSN 1573-2924. URL <https://doi.org/10.1007/s11081-023-09807-x>.

Picheny, V., Ginsbourger, D., Roustant, O., Haftka, R. T., and Kim, N.-H. Adaptive designs of experiments for accurate approximation of a target region. *Journal of Mechanical Design*, 132(071008), 2010. ISSN 1050-0472. URL <https://doi.org/10.1115/1.4001873>.

Picheny, V., Moss, H., Torossian, L., and Durrande, N. Bayesian quantile and expectile optimisation. In *Proceedings of the Thirty-Eighth Conference on Uncertainty in Artificial Intelligence*, pp. 1623–1633. PMLR, August 2022. URL <https://proceedings.mlr.press/v180/picheny22a.html>.

Qing, J., Couckuyt, I., and Dhaene, T. A robust multi-objective Bayesian optimization framework considering input uncertainty. *Journal of Global Optimization*, 86(3):693–711, July 2023. ISSN 1573-2916. URL <https://doi.org/10.1007/s10898-022-01262-9>.

Scott, W., Frazier, P. I., and Powell, W. B. The correlated knowledge gradient for simulation optimization of continuous parameters using Gaussian process regression. *SIAM Journal on Optimization*, 21(3):996–1026, 2011. URL <https://doi.org/10.1137/100801275>.

Sun, S., Li, X., Liu, H., Luo, K., and Gu, B. Fast statistical analysis of rare circuit failure events via scaled-sigma sampling for high-dimensional variation space. *IEEE Transactions on Computer-Aided Design of Integrated Circuits and Systems*, 34(7):1096–1109, 2015. ISSN 1937-4151. URL <https://doi.org/10.1109/TCAD.2015.2404895>.

Tabandeh, A., Jia, G., and Gardoni, P. A review and assessment of importance sampling methods for reliability analysis. *Structural Safety*, 97:102216, 2022. ISSN 0167-4730. URL <https://doi.org/10.1016/j.strusafe.2022.102216>.

Tong, S. and Stadler, G. Large deviation theory-based adaptive importance sampling for rare events in high dimensions. *SIAM/ASA Journal on Uncertainty Quantification*, 11(3):788–813, 2023. URL <https://doi.org/10.1137/22M1524758>.

Tsai, S. C., Park, C., and Chang, M. H. Metamodel-based simulation optimization considering a single stochastic constraint. *Computers & Operations Research*, 155:106239, 2023. ISSN 0305-0548. URL <https://doi.org/10.1016/j.cor.2023.106239>.

ur Rehman, S., Langelaar, M., and van Keulen, F. Efficient Kriging-based robust optimization of unconstrained problems. *Journal of Computational Science*, 5(6):872–881, November 2014. ISSN 1877-7503. URL <https://doi.org/10.1016/j.jocs.2014.04.005>.

Wang, M., Lv, W., Yang, F., Yan, C., Cai, W., Zhou, D., and Zeng, X. Efficient yield optimization for analog and

SRAM circuits via Gaussian process regression and adaptive yield estimation. *IEEE Transactions on Computer-Aided Design of Integrated Circuits and Systems*, 37(10):1929–1942, 2018. ISSN 1937-4151. URL <https://doi.org/10.1109/TCAD.2017.2778061>.

Weller, D. D., Hefenbrock, M., Beigl, M., and Tahoori, M. B. Fast and efficient high-sigma yield analysis and optimization using kernel density estimation on a Bayesian optimized failure rate model. *IEEE Transactions on Computer-Aided Design of Integrated Circuits and Systems*, 41(3):695–708, 2022. ISSN 1937-4151. URL <https://doi.org/10.1109/TCAD.2021.3064440>.

Wilson, J., Borovitskiy, V., Terenin, A., Mostowsky, P., and Deisenroth, M. Efficiently sampling functions from Gaussian process posteriors. In *Proceedings of the 37th International Conference on Machine Learning*, pp. 10292–10302. PMLR, 2020. URL <https://proceedings.mlr.press/v119/wilson20a.html>.

Wilson, J., Borovitskiy, V., Terenin, A., Mostowsky, P., and Deisenroth, M. Pathwise conditioning of Gaussian processes. *Journal of Machine Learning Research*, 22(105):1–47, 2021. ISSN 1533-7928. URL <http://jmlr.org/papers/v22/20-1260.html>.

A. Proofs of Theoretical Results

In this appendix we provide proofs of the theoretical results stated in the main text. We restate all results before proving them for convenience.

Lemma 2.1 (Formal Version). Suppose that $f : \mathcal{Y} \rightarrow \mathbb{R}$ is continuous and $\mathbf{g} : \mathcal{X} \times \mathcal{U} \rightarrow \mathcal{Y}$ is continuous. Suppose further that the distribution of $\mathbb{P}_{\mathbf{u}}$ has no mass on the limit state surface or boundary of $\mathcal{Y}_{\text{feas}}$, so that for any $\mathbf{x} \in \mathcal{X}$,

$$\begin{aligned}\mathbb{P}_{\mathbf{u}}(f \circ \mathbf{g}(\mathbf{x}, \mathbf{u}) = c) &= 0, \\ \mathbb{P}_{\mathbf{u}}(\mathbf{g}(\mathbf{x}, \mathbf{u}) \in \partial \mathcal{Y}_{\text{feas}}) &= 0.\end{aligned}$$

Then the failure probability $P : \mathcal{X} \rightarrow [0, 1]$ is continuous. If also \mathcal{X} is compact then P attains its minimum value for some $\mathbf{x}^* \in \mathcal{X}$.

Proof. Let $\mathbf{x} \in \mathcal{X}$ and let $\mathcal{S}_{\mathbf{x}}^{(1)} = \{\mathbf{u} \in \mathcal{U} : f \circ \mathbf{g}(\mathbf{x}, \mathbf{u}) = c\}$ and $\mathcal{S}_{\mathbf{x}}^{(2)} = \{\mathbf{u} \in \mathcal{U} : \mathbf{g}(\mathbf{x}, \mathbf{u}) \in \partial \mathcal{Y}_{\text{feas}}\}$ denote the components of the limit state surface for \mathbf{x} and let $\mathcal{S}_{\mathbf{x}} = \mathcal{S}_{\mathbf{x}}^{(1)} \cup \mathcal{S}_{\mathbf{x}}^{(2)}$. Then $\mathbb{P}(\mathbf{u} \in \mathcal{U} \setminus \mathcal{S}_{\mathbf{x}}) = 1$. Observe that

$$P(\mathbf{x}) = \mathbb{E}_{\mathbf{u}} \left[\mathbb{I}_{\{f \circ \mathbf{g}(\mathbf{x}, \mathbf{u}) \geq c\}} \mathbb{I}_{\{\mathbf{g}(\mathbf{x}, \mathbf{u}) \in \mathcal{Y}_{\text{feas}}\}} + \mathbb{I}_{\{\mathbf{g}(\mathbf{x}, \mathbf{u}) \notin \mathcal{Y}_{\text{feas}}\}} \right].$$

Let $\mathbf{u} \in \mathcal{U} \setminus \mathcal{S}_{\mathbf{x}}$ and let (\mathbf{x}_n) be a sequence in \mathcal{X} with $\mathbf{x}_n \rightarrow \mathbf{x}$ as $n \rightarrow \infty$. Then $f \circ \mathbf{g}(\cdot, \mathbf{u}) : \mathcal{X} \rightarrow \mathbb{R}$ is continuous and $f \circ \mathbf{g}(\mathbf{x}_n, \mathbf{u}) \rightarrow f \circ \mathbf{g}(\mathbf{x}, \mathbf{u})$ as $n \rightarrow \infty$. Further, since $f \circ \mathbf{g}(\mathbf{x}, \mathbf{u}) \neq c$, it follows $\mathbb{I}_{\{f \circ \mathbf{g}(\mathbf{x}_n, \mathbf{u}) \geq c\}}$ is eventually constant and so $\mathbb{I}_{\{f \circ \mathbf{g}(\mathbf{x}_n, \mathbf{u}) \geq c\}} \rightarrow \mathbb{I}_{\{f \circ \mathbf{g}(\mathbf{x}, \mathbf{u}) \geq c\}}$. Similarly, $\mathbf{g}(\mathbf{x}, \mathbf{u}) \notin \partial \mathcal{Y}_{\text{feas}}$ so by the same argument $\mathbb{I}_{\{\mathbf{g}(\mathbf{x}_n, \mathbf{u}) \in \mathcal{Y}_{\text{feas}}\}} \rightarrow \mathbb{I}_{\{\mathbf{g}(\mathbf{x}, \mathbf{u}) \in \mathcal{Y}_{\text{feas}}\}}$.

This holds for $\mathbb{P}_{\mathbf{u}}$ -almost every $\mathbf{u} \in \mathcal{U}$, so by the Dominated Convergence Theorem, $P(\mathbf{x}_n) \rightarrow P(\mathbf{x})$ and so P is continuous at \mathbf{x} . Since \mathbf{x} was arbitrary, P is everywhere continuous.

Finally, if \mathcal{X} is also compact, then as a continuous function on a compact set, P attains its minimum for some $\mathbf{x}^* \in \mathcal{X}$. \square

Before proving Lemma 5.1, we formally state the required regularity conditions.

Assumption A.1.

- a) For any $\mathbf{y}'_1, \dots, \mathbf{y}'_N \in \mathcal{Y}$ (not necessarily the points chosen during optimization) and any $v_1, \dots, v_N \in \mathcal{R}$, the set $\{\mathbf{y} \in \mathcal{Y} : \text{Var}[f(\mathbf{y}) \mid f(\mathbf{y}'_1) = v_1, \dots, f(\mathbf{y}'_N) = v_N] = 0\}$ has Lebesgue measure zero,
- b) For any $\mathbf{x} \in \mathcal{X}$, $\mathbf{g}(\mathbf{x}, \mathbf{u})$ (where $\mathbf{u} \sim \mathbb{P}_{\mathbf{u}}$) is absolutely continuous with respect to Lebesgue measure on \mathcal{Y} ,
- c) For any $\mathbf{x} \in \mathcal{X}$, $\mathbb{P}_{\mathbf{u}}(\mathbf{g}(\mathbf{x}, \mathbf{u}) \in \partial \mathcal{Y}_{\text{feas}}) = 0$.

The first of these assumptions ensures that the GP is sufficiently non-degenerate. Combined with the second assumption, this will be sufficient to deduce that $\mathbb{P}(f \circ \mathbf{g}(\mathbf{x}, \mathbf{u}) = c \mid \mathcal{F}_n) = 0$. That is, that $\mathbb{P}_{\mathbf{u}}$ and f jointly place no mass on the, now stochastic, limit state surface. Combined with the final part of Assumption A.1 these conditions are analogous to those in Lemma 2.1.

Lemma 5.1 (Formal Version). Suppose that f is a sample-continuous Gaussian process, that $\mathbf{g} : \mathcal{X} \times \mathcal{U} \rightarrow \mathcal{Y}$ is continuous and that Assumption A.1 holds. Then $P_n : \mathcal{X} \rightarrow [0, 1]$ is continuous. If also \mathcal{X} is compact then P_n attains its minimum value for some $\mathbf{x}_n^* \in \mathcal{X}$.

Proof. Write $(\Omega, \mathcal{F}, \mathbb{P})$ for the underlying probability space.

We will first show that, for all $\mathbf{x} \in \mathcal{X}$, $\mathbb{P}(f \circ \mathbf{g}(\mathbf{x}, \mathbf{u}) = c \mid \mathcal{F}_n) = 0$ almost surely. Indeed, the first two parts of Assumption A.1 give that for all $\mathbf{x} \in \mathcal{X}$, $\text{Var}[f \circ \mathbf{g}(\mathbf{x}, \mathbf{u}) \mid \mathbf{u}, \mathcal{F}_n] > 0$ almost surely. Thus, $f \circ \mathbf{g}(\mathbf{x}, \mathbf{u}) \mid \mathbf{u}, \mathcal{F}_n$ is an almost surely non-degenerate Gaussian random variable and hence $\mathbb{P}_{\mathbf{u}}(f \circ \mathbf{g}(\mathbf{x}, \mathbf{u}) = c \mid \mathbf{u}, \mathcal{F}_n) = 0$ almost surely. Therefore,

$$\mathbb{P}(f \circ \mathbf{g}(\mathbf{x}, \mathbf{u}) = c \mid \mathcal{F}_n) = \mathbb{E}[\mathbb{P}(f \circ \mathbf{g}(\mathbf{x}, \mathbf{u}) = c \mid \mathbf{u}, \mathcal{F}_n) \mid \mathcal{F}_n] = 0 \quad \text{a.s.}$$

The remainder of the proof follows that of Lemma 2.1.

Let $\mathbf{x} \in \mathcal{X}$, and define events $A = \{\omega \in \Omega : f(\mathbf{g}(\mathbf{x}, \mathbf{u}(\omega); \omega) \geq c\}$ and $B = \{\omega \in \Omega : \mathbf{g}(\mathbf{x}, \mathbf{u}(\omega)) \notin \mathcal{Y}_{\text{feas}}\}$. These are indeed events because f is sample-continuous (and so jointly measurable) and \mathbf{g} is continuous. Then $P_n(\mathbf{x}) = \mathbb{E}[\mathbb{I}_A(1 - \mathbb{I}_B) + \mathbb{I}_B | \mathcal{F}_n]$ is also well-defined.

Let (\mathbf{x}_m) be a sequence in \mathcal{X} with $\mathbf{x}_m \rightarrow \mathbf{x}$ as $m \rightarrow \infty$ and define events A_m and B_m as for A and B but with \mathbf{x}_m in place of \mathbf{x} . That is, $A_m = \{\omega \in \Omega : f(\mathbf{g}(\mathbf{x}_m, \mathbf{u}(\omega); \omega) \geq c\}$, $B_m = \{\omega \in \Omega : \mathbf{g}(\mathbf{x}_m, \mathbf{u}(\omega)) \notin \mathcal{Y}_{\text{feas}}\}$ and $P_n(\mathbf{x}_m) = \mathbb{E}[\mathbb{I}_{A_m}(1 - \mathbb{I}_{B_m}) + \mathbb{I}_{B_m} | \mathcal{F}_n]$.

Since \mathbf{g} is continuous, we conclude $f(\mathbf{g}(\cdot, \mathbf{u}))$ has almost surely continuous sample paths. Further, $\mathbb{P}(f(\mathbf{g}(\mathbf{x}, \mathbf{u})) = c | \mathcal{F}_n) = 0$ and so \mathbb{I}_{A_m} is almost surely eventually constant, and hence $\mathbb{I}_{A_m} \rightarrow \mathbb{I}_A$ as $m \rightarrow \infty$. A similar argument establishes that $\mathbb{I}_{B_m} \rightarrow \mathbb{I}_B$ almost surely, and so the Dominated Convergence Theorem gives $P_n(\mathbf{x}_m) \rightarrow P_n(\mathbf{x})$ as $m \rightarrow \infty$.

Finally, if \mathcal{X} is also compact, then as a continuous function on a compact set, P_n attains its minimum for some $\mathbf{x}_n^* \in \mathcal{X}$. \square

Lemma 6.3. *The KG-MR acquisition function in (10) is everywhere non-negative. That is,*

$$\forall n \geq 0 \quad \forall \mathbf{y} \in \mathcal{Y}_{\text{feas}} \quad \alpha_n^{\text{KG-MR}}(\mathbf{y}) \geq 0.$$

Proof. For all $\mathbf{x}' \in \mathcal{X}$

$$\begin{aligned} & \max_{\mathbf{x} \in \mathcal{X}} R_{n+1}(\mathbf{x}) \geq R_{n+1}(\mathbf{x}') \\ \Rightarrow \quad & \mathbb{E} \left[\max_{\mathbf{x} \in \mathcal{X}} R_{n+1}(\mathbf{x}) \mid \mathcal{F}_n, \mathbf{y}_{n+1} = \mathbf{y} \right] \geq \mathbb{E} [R_{n+1}(\mathbf{x}') \mid \mathcal{F}_n, \mathbf{y}_{n+1} = \mathbf{y}] \geq R_n(\mathbf{x}') \end{aligned}$$

where the last inequality follows from Jensen's inequality because $z \mapsto -\log z$ is convex. This holds for all \mathbf{x}' and so

$$\begin{aligned} & \mathbb{E} \left[\max_{\mathbf{x} \in \mathcal{X}} R_{n+1}(\mathbf{x}) \mid \mathcal{F}_n, \mathbf{y}_{n+1} = \mathbf{y} \right] \geq \max_{\mathbf{x} \in \mathcal{X}} R_n(\mathbf{x}) \\ \Rightarrow \quad & \alpha_n^{\text{KG-MR}}(\mathbf{y}) = \mathbb{E} \left[\max_{\mathbf{x} \in \mathcal{X}} R_{n+1}(\mathbf{x}) \mid \mathcal{F}_n, \mathbf{y}_{n+1} = \mathbf{y} \right] - \max_{\mathbf{x} \in \mathcal{X}} R_n(\mathbf{x}) \geq 0. \end{aligned}$$

\square

B. Optimization of the One-Shot Knowledge Gradient Approximations

We optimize the one-shot KG-MR acquisition function (14) using multi-start L-BFGS-B. Care must be taken when choosing starting locations for the multi-start optimization since the optimization landscape contains many local minima. Indeed, suppose that $\hat{R}_{n+1}(\mathbf{x}; \mathbf{y}, z_j)$ has m local minima in \mathbf{x} . Then the maximand on the right-hand side of (14) has m^{N_v} local minima in $\mathbf{x}_1, \dots, \mathbf{x}_{N_v}$, each with its own optimal \mathbf{y} .

In our experiments we adopt the following procedure to choose initial points. First, we evaluate the discrete KG-MR (15) at a large number N_{raw} of \mathbf{y} -values. We then choose N_{restarts} of these using Boltzmann sampling to randomly select starting locations which favor those with higher values. If the best value was not chosen, we replace the last sampled value with the best value. These values of \mathbf{y} and their corresponding $\mathbf{x}_1, \dots, \mathbf{x}_{N_v} \in \mathcal{X}_{\text{disc}}$ are used to initialize the multi-start L-BFGS-B optimization of (14). This implementation of Boltzmann sampling is standard within BoTorch.

C. Baseline Algorithms

In this appendix, we describe the algorithms which exist in the literature which were used as baselines.

C.1. The Method of Huang & Chan (2010)

Huang & Chan (2010) propose a Bayesian optimization method which chooses between four acquisition functions. If there are currently no feasible samples, then the probability of feasibility (17a) is optimized. Otherwise, three other acquisition functions are tried in order until one yields a point at least a distance ε_s from all existing samples. First (17b) is tried which seeks to maximize distance to existing observations while being within Δ of the predicted limit state surface. If that fails,

(17c) is maximized to seek new, disconnected areas of the limit state surface, known as tunneling. Finally, if all else fails, (17d) is optimized to seek the point with maximum variance and hence reduce uncertainty in the model. Listed together, the acquisition functions are,

$$\alpha_n^F(\mathbf{y}) = \mathbb{P}(f(\mathbf{y}) \leq c) = \Phi\left(\frac{c - \mu_n(\mathbf{y})}{\sqrt{k_n(\mathbf{y}, \mathbf{y})}}\right), \quad (17a)$$

$$\alpha_n^{LS}(\mathbf{y}) = \mathbb{I}_{\{|\mu_n(\mathbf{y}) - c| \leq \Delta\}} \min_{i=1, \dots, n} \frac{\|\mathbf{y}_i - \mathbf{y}\|}{\|\mathbf{b} - \mathbf{a}\|}, \quad (17b)$$

$$\alpha_n^{TN}(\mathbf{y}) = \alpha_n^F(\mathbf{y}) \min_{\substack{i=1, \dots, n \\ \text{s.t. } f(\mathbf{y}_i) \leq c}} \frac{\|\mathbf{y}_i - \mathbf{y}\|}{\|\mathbf{b} - \mathbf{a}\|}, \quad (17c)$$

$$\alpha_n^{MV}(\mathbf{y}) = \sqrt{k_n(\mathbf{y}, \mathbf{y})}. \quad (17d)$$

As before, here $\mathbf{y}_1, \dots, \mathbf{y}_n$ are the locations of the n observations made so far, and \mathbf{a}, \mathbf{b} define the bounds of the problem such that $\mathcal{Y}_{\text{feas}} = \prod_{j=1}^{d_y} [a_j, b_j]$. Note that in (17) we have kept the names from (Huang & Chan, 2010), but α_n^{MV} is a different acquisition function to the one used for TS-MR defined in Section 6.1.

We optimize the limit state exploration function α_n^{LS} from (17b) using DIRECT (Jones et al., 1993; Gablonsky & Kelley, 2001) and all other acquisition functions using multi-start L-BFGS-B. For numerical stability, we optimize the logarithm of (17a) rather than the acquisition function itself. In (Huang & Chan, 2010), the GP hyperparameters are fitted using a variogram, however for a fair comparison with the other algorithms, we use the same GP model and maximum a posteriori (MAP) estimation method for the hyperparameters for all algorithms. Rather than implementing the termination criteria from this work, we instead run the algorithm for the same fixed evaluation budget as the other algorithms for a fair comparison. In the experimental section, we denote this algorithm HC.

C.2. The Method of Bichon et al. (2008)

Bichon et al. (2012) propose a family of methods to tackle three problems in reliability-based design optimization, which include the problem posed in (1). The work extends their earlier work in active learning in which they proposed efficient global reliability analysis (EGRA) to efficiently estimate the failure probability (Bichon et al., 2008). They present three possible ways to combine BO with EGRA:

1. A nested approach using a separate surrogate for the function $\mathbf{u} \mapsto f(g(\mathbf{x}, \mathbf{u}))$ for each $\mathbf{x} \in \mathcal{X}$ visited,
2. A nested approach using a single surrogate to model $h(\mathbf{x}, \mathbf{u}) = f(g(\mathbf{x}, \mathbf{u}))$,
3. A sequential approach which alternates BO to find a good \mathbf{x} and EGRA to determine the limit state surface.

Their general formulation of the problem does not assume the composition $f(g(\mathbf{x}, \mathbf{u}))$ meaning the limit state surface could be different for different \mathbf{x} . However, in our case, the surface is essentially the same for each \mathbf{x} after an appropriate transform depending on g . Bichon et al. (2012) include such a problem in section 5.3 (steel column), and remark that the algorithms they propose are essentially identical in this case. Further, their formulation of the problem is a constrained optimization, with deterministic constraints coming from the original objective. At the first design point, a full EGRA analysis is performed, and subsequent design points are used to search the design space for points which satisfy these constraints using constrained BO. However, in the problem considered in this paper, (1) contains no constraints from an original objective. Therefore, to the best of our understanding, in the setting of (1) where there are no black-box constraints, the algorithm proposed in (Bichon et al., 2012) reduces to EGRA.

The EGRA algorithm was inspired by EI (Jones et al., 1998) and can be summarized as maximizing

$$\alpha_n^{\text{EGRA}}(\mathbf{y}) = \mathbb{E}\left[\max\left\{\epsilon - |c - f(\mathbf{y})|, 0\right\} \middle| \mathcal{F}_n\right] \quad (18)$$

where $\epsilon = \kappa \sqrt{k_n(\mathbf{y}, \mathbf{y})}$ is proportional to the marginal posterior standard deviation of f . Like HC, it explores the whole limit state surface, rather than concentrating on the parts contributing most to the failure probability at the point with maximal reliability.

To ensure a meaningful comparison, in the experiments we use the same GP model for all algorithms, with MAP estimated hyperparameters, rather than using either of the models from (Bichon et al., 2008) or (Bichon et al., 2012). For the value of κ , we use $\kappa = 2$ as recommended in Bichon et al. (2008; 2012). Bect et al. (2011) found a value of $\kappa = 0.5$ to give better

results for the estimation of failure probabilities, however for maximizing reliability we found little difference, as is shown in Figure 3.

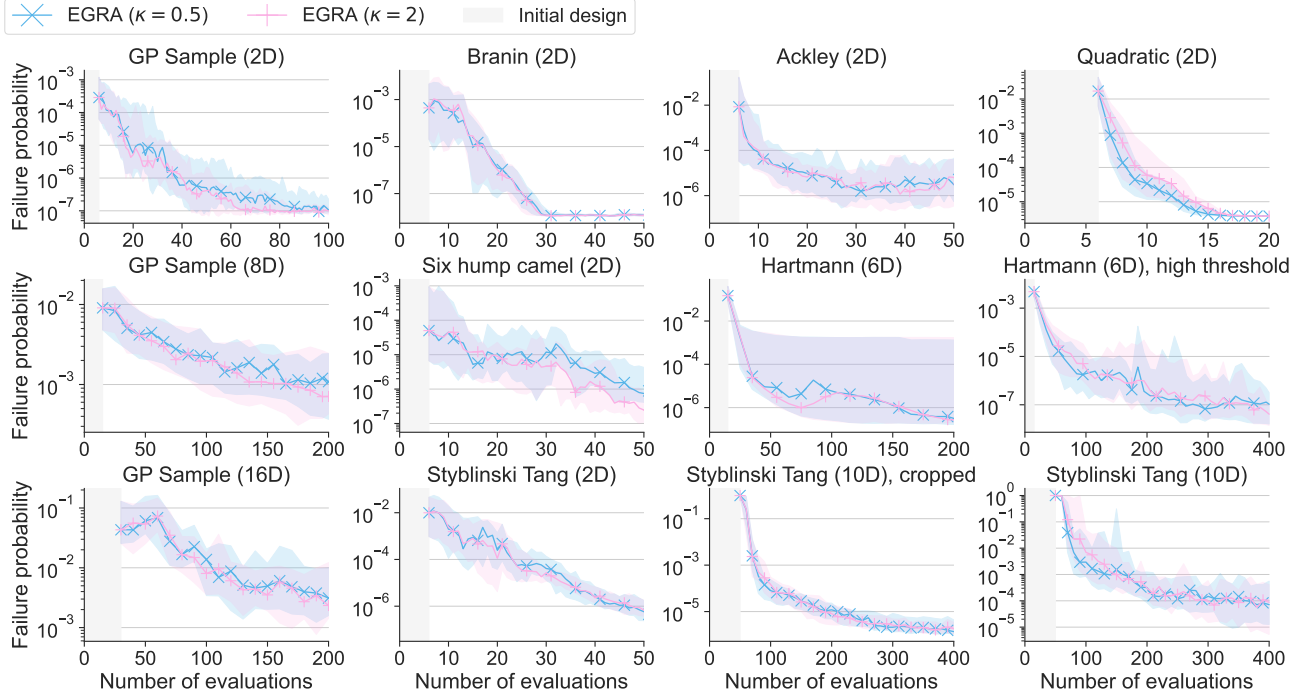


Figure 3. Failure probabilities of the two EGRA variants for the 12 test problems in Figure 2. The failure probability associated with the recommended solution is shown as a function of number of evaluations of the expensive black-box function. The solid lines show the median failure probability over 30 repeats and the shaded regions show the upper and lower quartiles.

D. Further Experimental Details

In this appendix, we give further details on the experimental procedure which is important for the reproduction of results but can be safely omitted on first reading.

D.1. Indicator Smoothing

In Section 7 we briefly introduced a smooth approximation to $\mathbb{I}_{\{g(\mathbf{x}, \mathbf{u}) \in \mathcal{Y}_{\text{feas}}\}}$ used to resolve the lack of differentiability in (11).

We wish to avoid evaluating f outside $\mathcal{Y}_{\text{feas}}$ because, for example, the black-box function may be given by a simulation which raises an error or gives outputs which violate the GP modeling assumption outside this region. Therefore, we use an asymmetric smoothing function $\iota(\mathbf{g}(\mathbf{x}, \mathbf{u}); \delta) \approx \mathbb{I}_{\{g(\mathbf{x}, \mathbf{u}) \in \mathcal{Y}_{\text{feas}}\}}$ which has a value of zero when $\mathbf{g}(\mathbf{x}, \mathbf{u}) \notin \mathcal{Y}_{\text{feas}}$ and builds smoothly inside the feasible region. Here $\delta > 0$ controls the width of the interval around the boundary affected by the smoothing. Figure 4 shows the contribution of this approximation to the probability of failure in one dimension.

The precise formula used for the bounds smoothing when $\mathcal{Y}_{\text{feas}} = \prod_{j=1}^{d_y} [a_j, b_j]$ is a hyperrectangle is

$$\iota(\mathbf{g}(\mathbf{x}, \mathbf{u}); \delta) = \prod_{j=1}^{d_y} G\left(\frac{g_j(\mathbf{x}, \mathbf{u}) - a_j}{\delta}\right) G\left(\frac{b_j - g_j(\mathbf{x}, \mathbf{u})}{\delta}\right) \quad (19)$$

where δ is a smoothing parameter controlling the width of the smoothing region, and where g_j is the function evaluating the j th component of \mathbf{g} . For $z \in (0, 1)$, the function $G(z) = F(z/1 - z)$ where $F(\cdot)$ is the cumulative density function of a Gamma distribution with shape parameter 0.5 and rate parameter 1. For $z \leq 0$ we define $G(z) = 0$ and for $z \geq 1$ we set $G(z) = 1$. This formula comes from considering the j th lower bound a_j to be a random variable $A_j = a_j + \delta \frac{Z_j}{1+Z_j}$ where $Z_j \sim \text{Gamma}(0.5, 1)$, and similarly for the upper bounds.

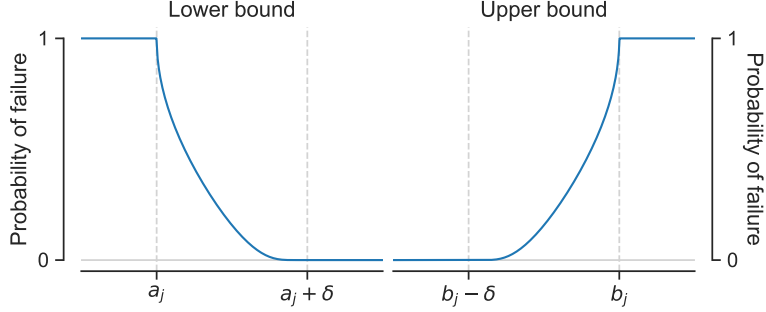


Figure 4. The approximation $1 - \nu(\mathbf{g}(\mathbf{x}, \mathbf{u}); \delta)$ of $\mathbb{I}_{\{\mathbf{g}(\mathbf{x}, \mathbf{u}) \notin \mathcal{Y}_{\text{feas}}\}}$ is shown as a function of $\mathbf{g}(\mathbf{x}, \mathbf{u})$. This is defined in (19) and used to smooth discontinuities in (11).

In practice, we keep δ very small, using a value of $\delta = \min(0.05\ell_{\min}, 0.1)$ where ℓ_{\min} is the minimum side-length of $\mathcal{Y}_{\text{feas}}$.

D.2. Model Parameters

For priors on the GP hyperparameters, we use $s^2 \sim \text{Gamma}(2, 0.15)$ for the output scale and $\ell_1, \dots, \ell_d \sim \text{Gamma}(3, 10)$. Here, gamma distributions are parametrized using the shape and rate convention. The constant mean has no prior (i.e. an improper prior) and variance of the observation noise is fixed to $\sigma^2 = 0.01^2$ for numerical stability. Actual observations $v_i = f(\mathbf{y}_i)$ have no noise added.

The GP hyperparameters are refitted every time a new observation is collected. Before fitting, we normalize and standardize the observations so that the inputs lie in $[0, 1]^{d_y}$ and the outputs have zero mean and unit variance. When making predictions with the GP, the inputs and outputs are transformed and untransformed appropriately. This is standard in BoTorch.

D.3. Optimizing the Recommendations

Recommendations \mathbf{x}_n^* ($n = 1, 2, \dots$) are generated from the GP surrogate using (12) for all algorithms. For the 2D problems, 10 restarts are chosen by evaluating the posterior mean on 1024 Sobol' points and using Boltzmann sampling, manually ensuring that the best found value is included as a start if necessary. These starting values are then optimized using L-BFGS-B. A qMC estimate with $N_u = 1024$ is used in (12c) and the bounds smoothing parameter δ in (12d) is set to $\delta = \min(0.05\ell, 0.1)$ where ℓ is the smallest side length in $\mathcal{Y}_{\text{feas}}$. A small nugget is added to the GP variance for numerical stability.

For the higher-dimensional problems (i.e. greater than 2D) the same is done, but the best value found is then fine-tuned with L-BFGS-B using a $N_u = 131,072$, since these problems benefit empirically from a larger value of N_u .

D.4. Test Problems

The test problems used, along with the threshold c and perturbation distribution $\mathbb{P}_{\mathbf{u}}$ are summarized in this section. All problems use additive perturbations, $\mathbf{g}(\mathbf{x}, \mathbf{u}) = \mathbf{x} + \mathbf{u}$.

BRANIN (2D)

The feasible domain is $\mathcal{Y}_{\text{feas}} = [-5, 10] \times [0, 15]$, the threshold is $c = 60$ and the formula is

$$f(\mathbf{y}) = \left(y_2 - \frac{5.1}{4\pi^2} y_1^2 + \frac{5}{\pi} y_1 - 6 \right)^2 + 10 \left(1 - \frac{1}{8\pi} \right) \cos(y_1) + 10. \quad (20)$$

The perturbation distribution is $\mathbb{P}_{\mathbf{u}} = \mathcal{N}(0, \text{diag}(0.8, 0.8)^2)$.

SIX HUMP CAMEL (2D)

The feasible domain is $\mathcal{Y}_{\text{feas}} = [-3, 3] \times [-2, 2]$, the threshold is $c = 2$ and the formula is

$$f(\mathbf{y}) = \left(4 - 2.1y_1^2 + \frac{1}{3}y_1^4\right)y_1^2 + y_1y_2 + 4(y_2^2 - 1)y_2^2. \quad (21)$$

The perturbation distribution is $\mathbb{P}_{\mathbf{u}} = \mathcal{N}(0, \text{diag}(0.2, 0.1)^2)$.

ACKLEY (2D)

The feasible domain is $\mathcal{Y}_{\text{feas}} = [-32.768, 32.768]^2$, the threshold is $c = 20.5$ and the formula is

$$f(\mathbf{y}) = -20 \exp\left(-0.2\sqrt{\frac{1}{2}(y_1^2 + y_2^2)}\right) - \exp\left(\frac{1}{2}[\cos(2\pi y_1) + \cos(2\pi y_2)]\right) + 20 + e. \quad (22)$$

The perturbation distribution is $\mathbb{P}_{\mathbf{u}} = \mathcal{N}(0, \text{diag}(3, 3)^2)$.

QUADRATIC (2D)

The feasible domain is $\mathcal{Y}_{\text{feas}} = [0, 1]^2$, the threshold is $c = 0.09$ and the formula is

$$f(\mathbf{y}) = (y_1 - 0.3)^2 + (y_2 - 0.3)^2. \quad (23)$$

The perturbation distribution is $\mathbb{P}_{\mathbf{u}} = \mathcal{N}(0, \text{diag}(0.06, 0.06)^2)$.

STYBLINSKI-TANG (2D, 10D)

Writing $d = 2, 10$ for the dimension, the feasible domain is $\mathcal{Y}_{\text{feas}} = [-5, 5]^d$. The formula is

$$f(\mathbf{y}) = \frac{1}{2} \sum_{i=1}^d (y_i^4 - 16y_i^2 + 5y_i). \quad (24)$$

For the 2D problem, the threshold is $c = -20$ and the perturbation distribution is $\mathbb{P}_{\mathbf{u}} = \mathcal{N}(0, \text{diag}(0.25, 0.5)^2)$. For the 10D problem, the threshold is $c = -300$ and the perturbation distribution is $\mathbb{P}_{\mathbf{u}} = \mathcal{N}(0, \text{diag}(0.4, 0.4, 0.4, 0.1, \dots, 0.1)^2)$. For the cropped version of the 10D problem, the feasible domain is reduced to $\mathcal{Y}_{\text{feas}} = [-5, 0] \times [-5, 5]^3 \times [-5, 0]^6$.

HARTMANN (6D)

The feasible domain is $\mathcal{Y}_{\text{feas}} = [0, 1]^6$ and the formula is

$$f(\mathbf{y}) = -\sum_{i=1}^4 \alpha_i \exp\left(-\sum_{j=1}^6 A_{ij}(y_j - P_{ij})^2\right) \quad (25)$$

where

$$\begin{aligned} \alpha &= (1 \quad 1.2 \quad 3 \quad 3.2)^T \\ \mathbf{A} &= \begin{pmatrix} 10 & 3 & 17 & 3.5 & 1.7 & 8 \\ 0.05 & 10 & 17 & 0.1 & 8 & 14 \\ 3 & 3.5 & 1.7 & 10 & 17 & 8 \\ 17 & 8 & 0.05 & 10 & 0.1 & 14 \end{pmatrix} \\ \mathbf{P} &= \begin{pmatrix} 0.1312 & 0.1696 & 0.5569 & 0.0124 & 0.8283 & 0.5886 \\ 0.2329 & 0.4135 & 0.8307 & 0.3736 & 0.1004 & 0.9991 \\ 0.2348 & 0.1451 & 0.3522 & 0.2883 & 0.3047 & 0.6650 \\ 0.4047 & 0.8828 & 0.8732 & 0.5743 & 0.1091 & 0.0381 \end{pmatrix}. \end{aligned}$$

For the standard version, the threshold is $c = -1$ and the perturbation distribution is $\mathbb{P}_{\mathbf{u}} = \mathcal{N}(0, \text{diag}(0.05, \dots, 0.05)^2)$. For the version with the high threshold, we use $c = -0.05$ with $\mathbb{P}_{\mathbf{u}} = \mathcal{N}(0, \text{diag}(0.07, \dots, 0.07)^2)$. The perturbation distribution is $\mathbb{P}_{\mathbf{u}} = \mathcal{N}(0, \text{diag}(0.05, \dots, 0.05)^2)$.

GP SAMPLE (2D, 8D, 16D)

The GP sample test problems were generated using a random Fourier feature approximation with 1024 Fourier features. The GP has zero mean and a Matérn-5/2 kernel. The output scale was 10 and the length scales were approximately $0.2\sqrt{d}$ to maintain the problem complexity with increasing dimension. The thresholds were set so that 33% of the volume of $\mathcal{Y}_{\text{feas}}$ is infeasible. The perturbation distribution was chosen as an isotropic Gaussian with scale chosen to achieve an appropriate optimal failure probability. The absolute values used are summarized in Table 1.

The feasible domain is $\mathcal{Y}_{\text{feas}} = [0, 1]^d$.

Table 1. Parameters used to generate the GP test problems.

Dimension	Isotropic length scale	Threshold, c	Failure volume	Perturbation distribution, $\mathbb{P}_{\mathbf{u}}$
2	0.28	3.6	33%	$\mathcal{N}(0, 0.04^2 \mathbf{I})$
8	0.57	1.2	33%	$\mathcal{N}(0, 0.06^2 \mathbf{I})$
16	0.8	0.6	33%	$\mathcal{N}(0, 0.07^2 \mathbf{I})$

D.5. Algorithm Parameters

For all experiments, the number of fantasies used in osKG-MR and dKG-MR is $N_v = 64$. The number of qMC points used for the expectation over \mathbf{u} in both KG-MR algorithms and in TS-MR is $N_u = 64$. For dKG-MR the size of the discretization $\mathcal{X}_{\text{disc}}$ is $N_x = 512$. Where importance sampling is used (i.e. for experiments with extreme failure probabilities), we use a scale factor of $\tau = 3$. The bounds smoothing parameter δ was set to $\min(0.05\ell_{\min}, 0.1)$ where ℓ_{\min} is the smallest side length of the feasible domain $\mathcal{Y}_{\text{feas}}$. The threshold smoothing parameter in TS-MR was set to $\rho = 0.01$. For EGRA, we use $\kappa = 2$ for most experiments, but $\kappa = 0.5$ in the sensitivity study in Figure 3 in Appendix C.2. Multi-start L-BFGS-B uses 10 restarts for the optimization of the acquisition function.

No guidance is given in (Huang & Chan, 2010) for how to set the parameters ε_s and Δ in the HC algorithm. We choose the minimum distance between points according to $\varepsilon_s = 0.01\ell_{\text{diagonal}}$ where ℓ_{diagonal} is the length of the diagonal of the feasible box $\mathcal{Y}_{\text{feas}}$. This allows the minimum distance to grow with the dimension of the problem, since higher-dimensional problems naturally contain more volume and larger distances. It also gives values in line with those used in (Huang & Chan, 2010) where this value is reported. For the parameter Δ describing the width of the region of interest around the limit state surface, no values are reported in (Huang & Chan, 2010) and so we adopt a best-effort approach. Being a measure in objective space, intuitively the value of Δ used should scale with the gradient $\|\nabla f\|$ around the limit state surface. For the 2D problems, we plotted the landscape and chose a value of Δ to give a thin band around the limit state surface based on the contours. For higher-dimensional problems, we chose an appropriate value using either the formula (in the case of Hartmann and Styblinski-Tang) or the histogram of function values (in the case of the GP problems). Of course, this choice method would not be possible for a real black-box problem, and conveys an unfair advantage on the HC algorithm in our experiments. However, since HC is largely beaten by KG-MR and TS-MR, this does not invalidate the conclusions of the comparison. The parameters used for HC and the size n_0 of the initial design used by all algorithms are given in Table 2.

The parameters used when generating recommendations are specified in Appendix D.3.

E. Example Query Patterns

Figures 5 and 6 show the first 30 samples collected by the five algorithms tested on the 2D GP and six hump camel test problems. The osKG-MR and TS-MR algorithms clearly focus on the relevant part of the limit state surface, while the HC and EGRA algorithms sometimes initially focus on the wrong parts. In one case, HC fails to discover all disconnected parts of the limit state surface. The HC and EGRA algorithms also attempt to sample on the boundary $\partial\mathcal{Y}_{\text{feas}}$ in places where the value of f is close to the threshold c . This phenomenon been observed in other works on robust Bayesian optimization (Qing et al., 2023) where the algorithm cannot efficiently reduce the uncertainty in the GP outside the boundary. KG-MR and TS-MR naturally incorporate knowledge that perturbed solutions $\mathbf{y} \in \mathcal{Y} \setminus \mathcal{Y}_{\text{feas}}$ beyond the boundary will be infeasible and so do not suffer from this.

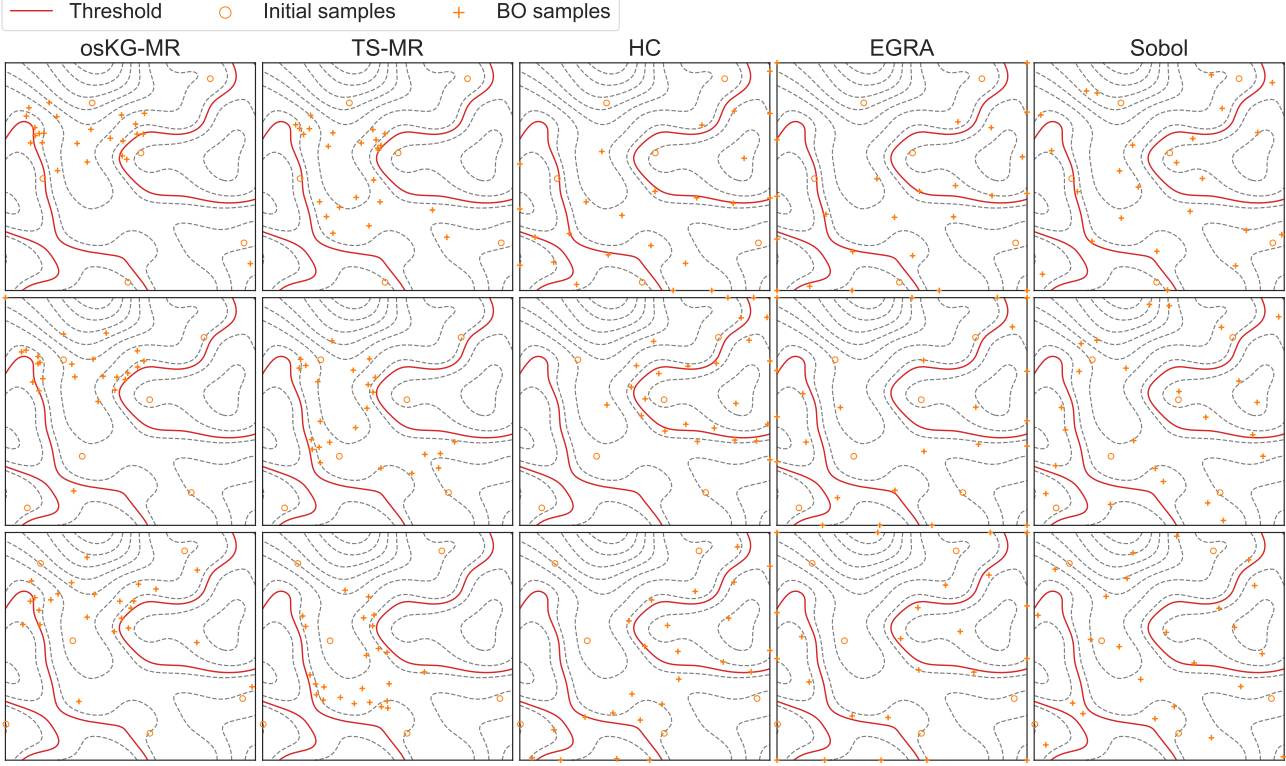


Figure 5. The first 30 sampling locations for five algorithms tested on the 2D GP test problem. The rows show three different runs, corresponding to three different initial designs.

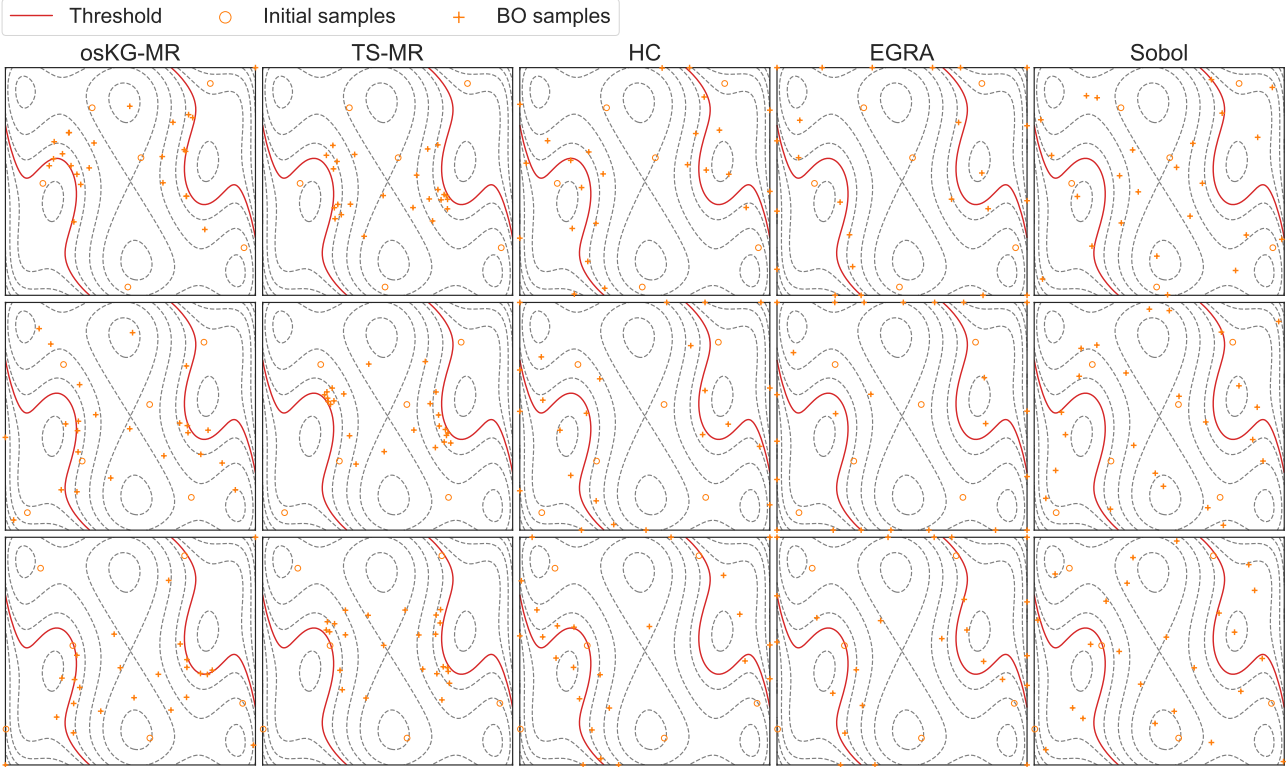


Figure 6. The first 30 sampling locations for five algorithms tested on the six hump camel test problem. The rows show three different runs, corresponding to three different initial designs.

Table 2. Experiment-specific parameters for the algorithms. For HC, these are the minimum distance between samples ε_s and the distance in objective space Δ defining the band of interest around the limit state surface. Additionally, the size n_0 of the initial design is used by all algorithms.

Experiment	HC		
	n_0	ε_s	Δ
GP (2D)	6	0.014	0.6
GP (8D)	15	0.028	0.6
GP (16D)	30	0.04	0.6
Branin (2D)	6	0.21	10
Six hump camel (2D)	6	0.072	0.4
Styblinski-Tang (2D)	6	0.14	10
Ackley (2D)	6	0.93	0.2
Quadratic (2D)	6	0.014	0.01
Hartmann (6D)	15	0.024	0.02
Hartmann (6D), high threshold	15	0.024	0.02
Styblinski-Tang (10D)	50	0.32	10
Styblinski-Tang (10D), cropped	50	0.22	10

F. Acquisition Function Timings

It is important when choosing an acquisition function to be aware of the time required to optimize the acquisition function, since this should be small compared with the time or cost required to evaluate the black-box function f . Tables 3 and 4 show the lower and upper quartiles of the time required to optimize the acquisition function for the problems in the middle two columns of Figure 2. These are not presented as a means to claim one algorithm is better than another, but rather to give an idea for how expensive the expensive black-box function f should be. For example, if evaluations of f take of the order of an hour then spending a 30s to optimize the one-shot KG-MR for the cropped, 10D Styblinski-Tang problem would be negligible.

The KG-MR algorithms, and in particular the one-shot KG-MR, are computationally intensive, and thus for problems with $d > 2$ they are run using a GPU while all other algorithm-problem combinations are run only using CPUs. The GPU used is an NVIDIA L40 (48GB RAM), and is paired with 10 cores from an AMD 9354P Genoa (Zen 4) processor and 59GB RAM. For the CPU only experiments, 8 cores of an Intel Xeon Platinum 8268 (Cascade Lake) processor are used with 19.6GB RAM.

Table 3. Lower and upper quartiles of the time required to optimize the acquisition functions on the 2D test problems from the middle two columns of Figure 2 at several points during the optimization. The value of n denotes the number of the sample currently being optimized. On the 2D test problems, all algorithms were run using 8 CPUs and a total of 29.6GB RAM.

		Ackley (2D)	Branin (2D)	Six hump camel (2D)	Styblinski Tang (2D)
Discrete KG-MR	$n = 7$	19s-23s	16s-19s	15s-19s	17s-19s
	$n = 50$	25s-33s	9s-65s	7s-14s	8s-30s
One-shot KG-MR	$n = 7$	21s-30s	24s-33s	20s-27s	23s-27s
	$n = 50$	27s-38s	9s-23s	25s-35s	22s-35s
TS-MR	$n = 7$	1.0s-1.3s	0.9s-1.1s	1.2s-2.2s	1.0s-1.4s
	$n = 50$	1.4s-1.5s	1.7s-2.0s	2.3s-2.7s	1.6s-2.0s
HC	$n = 7$	17s-23s	16s-24s	19s-29s	15s-24s
	$n = 50$	9s-12s	8s-11s	11s-14s	12s-15s
EGRA	$n = 7$	0.34s-0.44s	0.29s-0.45s	0.29s-0.44s	0.31s-0.50s
	$n = 50$	0.46s-0.58s	0.98s-1.43s	0.46s-0.66s	0.55s-0.77s

Table 4. Lower and upper quartiles of the time required to optimize the acquisition functions on the higher-dimensional test problems from the middle two columns of Figure 2 at several points during the optimization. The value of n denotes the number of the sample currently being optimized. On these test problems, the KG-MR algorithms were run using a GPU (NVIDIA L40 48 GB RAM) and 10 CPUs with a total of 59GB RAM. The remaining test problems use 8 CPUs and a total of 29.6GB RAM.

		Hartmann (6D)	Styblinski Tang (10D), cropped
Discrete KG-MR (GPU)	$n = 16$	1.6s-2.3s	
	$n = 100$	2.2s-4.4s	2.4s-4.3s
	$n = 200$	2.4s-7.1s	2.8s-6.0s
One-shot KG-MR (GPU)	$n = 16$	17s-26s	
	$n = 100$	27s-39s	25s-38s
	$n = 200$	28s-44s	29s-37s
TS-MR	$n = 16$	1.6s-3.3s	
	$n = 100$	4.2s-5.9s	1.9s-2.8s
	$n = 200$	4.6s-5.8s	2.6s-3.5s
HC	$n = 16$	1s-13s	
	$n = 100$	2.2s-2.9s	1s-11s
	$n = 200$	1.9s-3.4s	1.6s-4.2s
EGRa	$n = 16$	1.2s-3.6s	
	$n = 100$	1.5s-2.0s	1.7s-2.5s
	$n = 200$	1.5s-2.2s	2.3s-4.3s

G. Problems with Less Extreme Optimal Failure Probabilities

To complement the problem from the main paper, we also study the algorithms on problems where the optimal failure probability is not as extreme. In this case, we do not need importance sampling and also drop the logarithm from the definition of KG-MR. That is, we use $R_n(\mathbf{x}) = P_n(\mathbf{x})$ instead of Equation (6).

To achieve non-extreme optimal failure probabilities, the GP test problems were modified so that the proportion of $\mathcal{Y}_{\text{feas}}$ which is a failure increases with dimension. Additionally the standard deviation of the Gaussian perturbations was increased to 0.1. The kernel and random seed used to generate the problems was not changed, so the actual sample f remained the same. These changes are summarized in Table 5. For the non-GP test problems, the threshold was kept the same but the standard deviation of the noise variance was increased to the values shown in Table 6.

The results are shown in Figure 7. The conclusions are similar to the extreme case in Figure 2, with some exceptions. EGRa shows improved performance in the GP problems, while osKG-MR now matches the performance of EGRa on the (uncropped) Styblinski-Tang (10D) problem. TS-MR fails to converge to the same optimum as the other algorithms on the Styblinski-Tang (2D) problem. Generally, all algorithms converge faster, since the higher-variance perturbation distribution means that the failure probability landscape is simpler and less affected by small perturbations in the limit state surface.

Table 5. Parameters used to generate the GP test problems with non-extreme failure probabilities.

Dimension	Threshold, c	Failure volume	Perturbation distribution, \mathbb{P}_u
2	3.6	33%	$\mathcal{N}(0, 0.1^2 \mathbf{I})$
8	-1.4	67%	$\mathcal{N}(0, 0.1^2 \mathbf{I})$
10	-4.5	90%	$\mathcal{N}(0, 0.1^2 \mathbf{I})$

Table 6. Perturbation distributions used for the non-GP test problems with non-extreme failure probabilities

Problem	Perturbation distribution
Branin (2D)	$\mathcal{N}(0, 2.5^2 \mathbf{I})$
Six hump camel (2D)	$\mathcal{N}(0, \text{diag}(0.6, 0.3)^2)$
Styblinski-Tang (2D)	$\mathcal{N}(0, \text{diag}(1, 2)^2)$
Ackley (2D)	$\mathcal{N}(0, 8^2 \mathbf{I})$
Quadratic (2D)	$\mathcal{N}(0, 0.12^2 \mathbf{I})$
Hartmann (6D)	$\mathcal{N}(0, 0.1^2 \mathbf{I})$
Hartmann (6D), high threshold	$\mathcal{N}(0, 0.18^2 \mathbf{I})$
Styblinski-Tang (10D)	$\mathcal{N}(0, \text{diag}(0.8, 0.8, 0.8, 0.2, \dots, 0.2)^2)$
Styblinski-Tang (10D), cropped	$\mathcal{N}(0, \text{diag}(0.8, 0.8, 0.8, 0.2, \dots, 0.2)^2)$

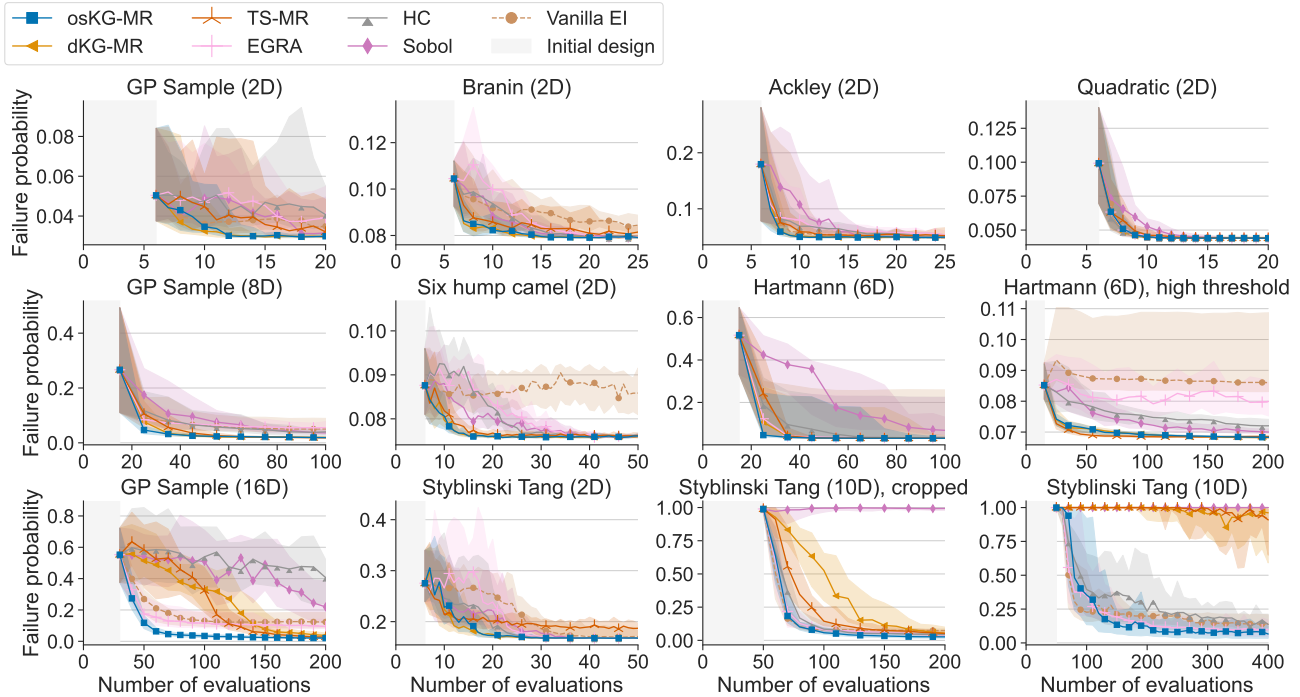


Figure 7. Failure probabilities for the 12 test problems with a non-extreme optimal failure probability. As for Figure 2, the first column contains the GP test problems, while the remaining columns are problems with potential for model mismatch. The last column contains problems for which KG-MR is not expected to have an advantage. The failure probability associated with the recommended solution is shown as a function of number of evaluations of the expensive black-box function. The solid lines show the median failure probability over 30 repeats and the shaded regions show the upper and lower quartiles.

H. Sensitivity Study

This section contains a study on the sensitivity of the one-shot and discrete KG-MR approximations to their parameters. The parameters studied are:

- the number N_u of qMC points used to estimate the expectation \mathbb{E}_u ,
- the number N_v of qMC points used to estimate the expectation over the next potential sample v_{n+1} ,
- the number $N_x = |\mathcal{X}_{\text{disc}}|$ of points in the discretization of \mathcal{X} (dKG-MR only),
- the number N_{restarts} of restarts used when optimizing the acquisition function with L-BFGS-B.

Sensitivity is tested on the problems in the middle two columns of Figure 2 and results are presented in Figures 8 and 9. Both algorithms are reasonably robust to all parameters. However,

- dKG-MR is sensitive to the size of N_x in the cropped 10D Styblinski-Tang problem,
- a higher N_u has a small benefit to osKG-MR in the cropped 10D Styblinski-Tang,
- a lower N_v is slightly harmful to osKG-MR in the Hartmann (6D) problem.

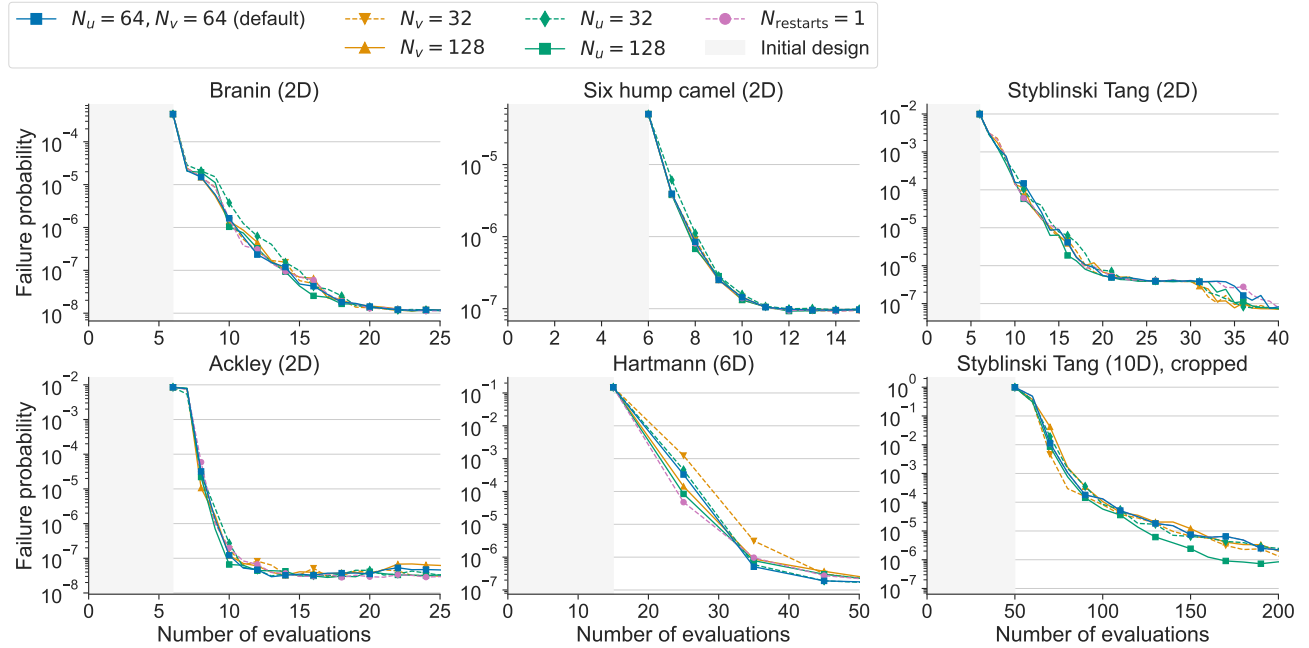


Figure 8. Sensitivity analysis on the one-shot KG-MR approximation (osKG-MR) on the problems with extremely small optimal failure probabilities in the middle two columns of Figure 2. The failure probability associated with the recommended solution is shown as a function of the number of evaluations of the expensive black-box function. The solid lines show the median failure probability over 30 repeats. The upper and lower quartiles are omitted for clarity. Only parameters which differ from the default are shown in the legend.

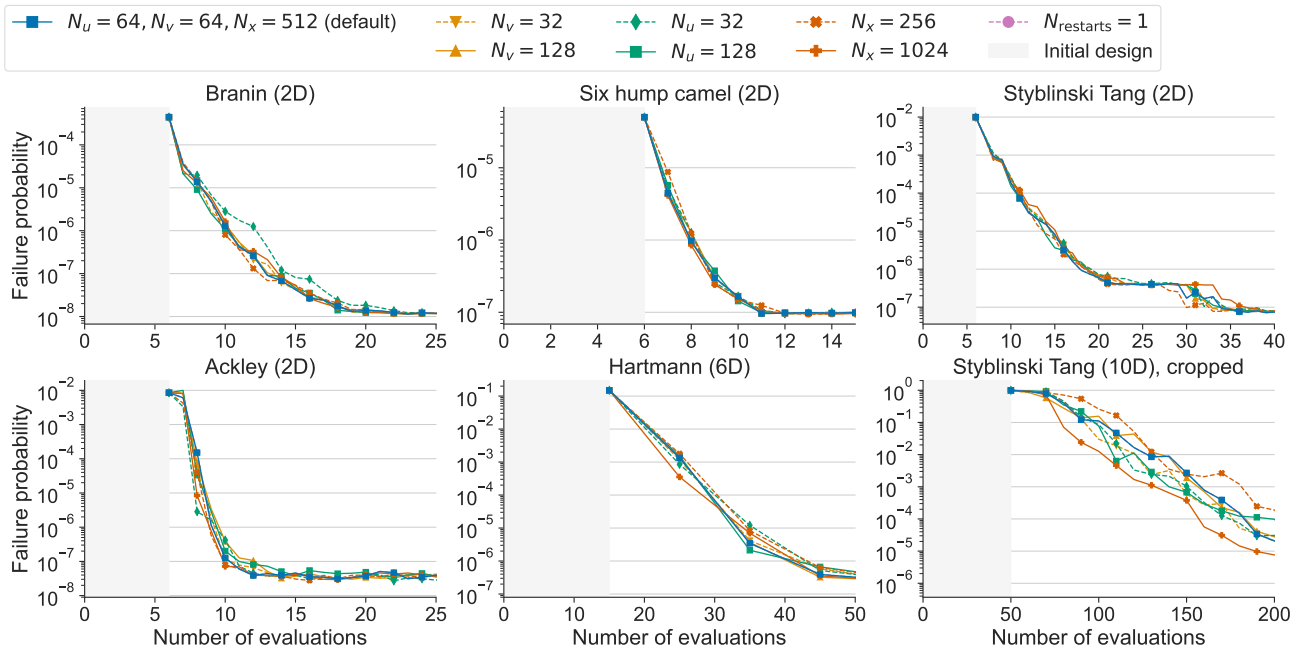


Figure 9. Sensitivity analysis on the discrete KG-MR approximation (dKG-MR) on the problems with extremely small optimal failure probabilities in the middle two columns of Figure 2. The failure probability associated with the recommended solution is shown as a function of the number of evaluations of the expensive black-box function. The solid lines show the median failure probability over 30 repeats. The upper and lower quartiles are omitted for clarity. Only parameters which differ from the default are shown in the legend.